

---

# Provable Stochastic Optimization for Global Contrastive Learning: Small Batch Does Not Harm Performance

---

Zhuoning Yuan<sup>1</sup>, Yuexin Wu<sup>2</sup>, Zihao Qiu<sup>3</sup>, Xianzhi Du<sup>2</sup>,  
 Lijun Zhang<sup>3</sup>, Denny Zhou<sup>2</sup>, Tianbao Yang<sup>1\*</sup>

<sup>1</sup>Department of Computer Science, the University of Iowa

<sup>2</sup>Google Research

<sup>3</sup>National Key Laboratory for Novel Software Technology, Nanjing University

## Abstract

In this paper, we study contrastive learning from an optimization perspective, aiming to analyze and address a fundamental issue of existing contrastive learning methods that either rely on a large batch size or a large dictionary. We consider a global objective for contrastive learning, which contrasts each positive pair with all negative pairs for an anchor point. From the optimization perspective, we explain why existing methods such as SimCLR requires a large batch size in order to achieve a satisfactory result. In order to remove such requirement, we propose a memory-efficient Stochastic Optimization algorithm for solving the Global objective of Contrastive Learning of Representations, named SogCLR. We show that its optimization error is negligible under a reasonable condition after a sufficient number of iterations or is diminishing for a slightly different global contrastive objective. Empirically, we demonstrate that on ImageNet with a batch size 256, SogCLR achieves a performance of 69.4% for top-1 linear evaluation accuracy using ResNet-50, which is on par with SimCLR (69.3%) with a large batch size 8,192. We also attempt to show that the proposed optimization technique is generic and can be applied to solving other contrastive losses, e.g., two-way contrastive losses for bimodal contrastive learning.

## 1 Introduction

Recently, self-supervised learning (SSL) for pre-training deep neural networks, which springs from natural language processing [24, 9, 20], has emerged to be a popular paradigm in computer vision for learning visual representations [10, 38, 22]. A simple yet effective framework of SSL for learning visual representations is contrastive learning [6, 2], which uses the gradient of a contrastive loss to update model, aiming to push the similarity scores between positive pairs (augmented data from the same image) to be higher than that between negative pairs (augmented data from different images).

While great performance of contrastive learning methods and their alternatives have been demonstrated on popular benchmarks (e.g., ImageNet), some fundamental problems of contrastive learning remain unresolved. One such problem is the requirement of large batch size. Unlike supervised learning methods, the performance of SimCLR [2] decreases as the batch size decreases, and a satisfactory performance can be only achieved with a large batch size on natural image datasets (e.g., 8192 for ImageNet). However, in practice, training models with such a large batch size can be memory-intensive and requires more computational resources, especially when adopting large-scale backbones (e.g., Vision Transformers [11, 36]) or taking video sequences as input [28].

---

\*Correspondence to zhuoning-yuan@uiowa.edu, dennyzhou@google.com, tianbao-yang@uiowa.edu. The code for experiments is available at <https://github.com/0ptimization-AI/sogclr>.

To address this issue, some ad-hoc approaches have been investigated. For example, the MoCo method [16] uses a large dictionary to maintain a set of feature vectors for constructing negative pairs with data in the mini-batch. Other approaches choose to get around such issue by optimizing pairwise loss [12] or other losses [35]. Nevertheless, the fundamental issue of optimizing a contrastive loss with a large batch size requirement still exists. This also occurs to other tasks with a similar contrastive loss, e.g., bimodal self-supervised learning tasks by optimizing a two-way contrastive loss (e.g., CLIP [29]).

In this paper, we aim to address this fundamental problem from the optimization perspective by considering a global objective for contrastive learning, providing a rigorous analysis to explain why SimCLR requires a large mini-batch size, and designing a memory-efficient stochastic algorithm for optimizing the global contrastive objective with provable convergence guarantee under a reasonable condition. Our major contributions are summarized below:

- We propose a global objective for contrastive learning, in which the similarity score between a random positive pair of an anchor point is contrasted with that between the anchor point and all other images and their augmented data. We cast the problem as a special case of coupled compositional stochastic optimization by highlighting the challenges in designing stochastic algorithms.
- We analyze SimCLR from the perspective of optimizing the global contrastive objective, and show that it suffers from an optimization error of SimCLR in the order of  $O(1/\sqrt{B})$  for the objective’s gradient norm even with the number of iterations approaching infinity, which explains the phenomena that SimCLR’s performance degrades as the mini-batch size decreases.
- We propose a memory-efficient stochastic algorithm named SogCLR without relying a large batch size. We establish the convergence of the proposed algorithm SogCLR and show that its optimization error for the aforementioned global contrastive objective is negligible under a mild condition. Moreover, we show that SogCLR converges to a stationary solution to a slightly different global contrastive objective with a diminishing optimization error as the number of iterations increases.
- We demonstrate the empirical success of SogCLR on ImageNet-1K data. With a standard mini-batch size 256, by running 800 epochs, SogCLR achieves a performance of 69.4% for top 1 linear evaluation accuracy, which is better than 69.3% of SimCLR using a large batch size 8,192. We further demonstrate the usefulness of the proposed technique for bimodal contrastive learning, e.g., CLIP.

Finally, we would like to emphasize that to the best of our knowledge, this is the first work that analyzes SimCLR and a stochastic algorithm for contrastive learning from an optimization perspective. We expect that this paper would inspire new studies by proposing better algorithms for optimizing the global contrastive objective.

## 2 Related Work

We would like to point out that self-supervised learning is an emerging field and there are tremendous studies proposing different methodologies. Nevertheless, we focus our attention on different methodologies for contrastive self-supervised learning.

**Contrastive Losses.** There are multiple definitions of contrastive loss, including pairwise losses, and listwise losses. The notation of contrastive loss dates back to 15 years ago for dimensionality reduction [15], which uses pairwise contrastive losses that simply pushes the similarity scores between positive pairs to be high and that between negative pairs to be low. Listwise contrastive losses have been proposed in the context of distance metric learning [30], which contrasts a similarity score between an anchor point and a positive sample with a number of similarity scores between the anchor point and multiple negative samples. [26] is a pioneering work that uses a contrastive loss for unsupervised representation learning. They propose a contrastive loss based on noise contrastive estimation (NCE), which is called InfoNCE. It was used to learn representations by predicting the future in the latent space by using autoregressive model. NCE was originally proposed for approximately maximizing log-likelihood of a complex probabilistic model with normalization term uncomputable. However, a fundamental issue regarding how to select the negative samples and how it affects the learning performance is not studied.

**Evolution of State-of-the-art.** The InfoNCE loss was later adopted in the momentum contrast (MoCo) method [16] for self-supervised learning of visual representations. MoCo tackles the question of how to construct negative samples in the latent space. It introduces two techniques (i) a momentum encoder network, which is used to generate representations of images for contrast with that generated by the target network on the anchor points, and is updated by a momentum step; (ii) a large dictionary that stores a number of feature representations for constructing negative pairs that are generated by the momentum encoder network, and is updated by a queue structure in a FIFO fashion. Later, the large dictionary and momentum contrast was abandoned in SimCLR [2], which uses a large batch to sample data for constructing positive and negative pairs within the batch. SimCLR makes several contributions for improving the performance, in particular using strong data augmentations and MLP projection layers. SimCLR conducted extensive experiments by studying how the batch size and other factors (e.g. number of epochs) affect the performance and a key observation is that the performance degrades as the mini-batch size decreases. Although a large-batch size is preferred or not an issue in industrial setting, the fundamental issue of requiring large batch size is still not well addressed. MoCo-v2 [4] uses strong data augmentations and MLP projection layers in the MoCo framework and improves the top-1 linear evaluation accuracy on ImageNet from 69.3% of SimCLR to 71.1% by using a ResNet-50 backbone.

The performance of top-1 linear evaluation accuracy was further improved in several works [1, 12, 25, 5, 31]. For example, [1] uses clustering assignment (codes) and prediction probabilities over clusters based on learned features to define a cross-entropy loss, where the clustering assignments of each sample are computed online using the prototype vectors and the learned representations. They also use a large dictionary to store a number of feature representations for finding the prototype vectors. Another useful trick in the paper is the multi-crop augmentation strategy. [12] uses the online/target network setup to define a simple pairwise loss, where the target network is updated by a momentum step similar to that used in MoCo. With a larger number of hidden nodes in MLP layers, their top-1 linear evaluation accuracy is 74.3% using a ResNet-50 backbone. Recently, [31] attains state-of-the-art performance of top-1 linear evaluation accuracy (77.1%) by using a combination of techniques, e.g., the contrastive loss as in SimCLR, the online-target setup as in [12], the multi-crop augmentations as in [1], and the invariance loss as in [25]. We also notice that larger backbones lead to better performance, e.g., ResNet-200 [12, 31] and Vision Transformer [5, 21]. We would like to point out that it is not our focus to leverage these different techniques to achieve state-of-the-art performance. But instead we focus on understanding the fundamental limits of optimizing the listwise contrastive loss and providing an alternative yet effective strategy to make contrastive learning possible without using a large batch size, which is potentially useful for different methods, e.g., supervised contrastive learning [19], and bimodal contrastive learning mentioned below [29].

**Global Contrastive Loss.** The challenge of handling a large number of components in the normalization term of softmax function is not well addressed. One of the most well-known techniques to address this challenge is to use NCE [14], which reduces the problem to how to sample negative data and how many negative data are sufficient for obtaining satisfactory performance. Although the original paper of NCE shows that the approximation error of NCE decreases as the number of samples increases, it is unclear how it affects the performance of SSL for visual representations. In contrast, this paper provides arguable better approach for tackling the global contrastive loss in the sense that (i) the performance does not hinge on how to sample negative samples and how many to sample; (ii) there is stronger convergence guarantee for optimizing the global contrastive loss.

**Bimodal Contrastive Learning.** Recently, a two-way contrastive loss has been used in bimodal contrastive learning [37, 29], which takes paired image and text as input and aims to map them into an Euclidean space that are closer than non-observed image/text pairs. The CLIP model [29] uses this idea to train a model on a large image-text dataset and observe promising zero-shot prediction performance for downstream tasks. However, their approach also uses a very large batch size equal to 32,768.

### 3 Optimizing Global Contrastive Objective

**Notations.** Let  $\mathcal{D} = \{\mathbf{x}_1, \dots, \mathbf{x}_n\}$  denote the set of training images, let  $\mathcal{P}$  denote a set of data augmentation operators that can be applied to each image to generate a copy. Let  $\mathcal{A}(\cdot) \in \mathcal{P}$  denote a random data augmentation operator, and let  $\mathbf{x} \in \mathcal{D}$  denote a random example from  $\mathcal{D}$ . Let  $\mathcal{S}_i = \{\mathcal{A}(\mathbf{x}) : \forall \mathcal{A} \in \mathcal{P}, \forall \mathbf{x} \in \mathcal{D} \setminus \{\mathbf{x}_i\}\}$  denote all training images including their augmented

versions but excluding that of  $\mathbf{x}_i$ . Let  $E(\cdot)$  denote the encoder network parameterized by  $\mathbf{w} \in \mathbb{R}^d$  that outputs a normalized feature representation of an input image. Below,  $\mathcal{A}(\mathbf{x}_i)$  and  $\mathcal{A}'(\mathbf{x}_i)$  denote two independent random data augmentations applied to  $\mathbf{x}_i$  and  $\mathbf{x}_j$  independently.

The SimCLR method is to update the model according to the gradient of the local contrastive loss that is defined over sampled mini-batch data. To this end, a random mini-batch of  $B$  images  $\mathcal{B} = \{\mathbf{x}_1, \dots, \mathbf{x}_B\}$  are first sampled. Then for each image  $\mathbf{x}_i \in \mathcal{B}$ , two random augmented data  $\mathcal{A}(\mathbf{x}_i), \mathcal{A}'(\mathbf{x}_i)$  are generated by two randomly sampled data augmentations  $\mathcal{A}, \mathcal{A}' \in \mathcal{P}$ . Then the gradient is computed based on the following local contrastive loss for each data  $\mathbf{x}_i$  and its symmetric one by switching  $\mathcal{A}$  and  $\mathcal{A}'$ :

$$L_{\mathcal{B}}(\mathbf{w}; \mathbf{x}_i, \mathcal{A}, \mathcal{A}') = -\ln \frac{\exp(E(\mathcal{A}(\mathbf{x}_i))^{\top} E(\mathcal{A}'(\mathbf{x}_i)) / \tau)}{g(\mathbf{w}; \mathbf{x}_i, \mathcal{A}, \mathcal{B})}, \quad (1)$$

where  $\tau$  is known as the temperature parameter, and

$$g(\mathbf{w}; \mathbf{x}_i, \mathcal{A}, \mathcal{B}_i) = \sum_{\mathbf{z}_j \in \mathcal{B}_i} (\exp(E(\mathcal{A}(\mathbf{x}_i))^{\top} E(\mathbf{z}_j) / \tau)) \quad (2)$$

and  $\mathcal{B}_i = \{\mathcal{A}(\mathbf{x}_j), \mathcal{A}'(\mathbf{x}_j) : \mathbf{x}_j \in \mathcal{B} \setminus \{\mathbf{x}_i\}\}$  denote the set of images that are generated by applying independent two random data augmentations to each image in  $\mathcal{B}$  independently excluding  $\mathbf{x}_i$ .

### 3.1 A Global Contrastive Objective: V1

The local contrastive loss defined over the mini-batch samples hides the complexity for contrastive learning, which renders the SimCLR method sensitive to the mini-batch size. To address this issue, we propose a global contrastive objective. To this end, we define the following global contrastive loss for each augmented data pair  $(\mathcal{A}(\mathbf{x}_i), \mathcal{A}'(\mathbf{x}_i))$ :

$$L(\mathbf{w}; \mathbf{x}_i, \mathcal{A}, \mathcal{A}') = -\ln \frac{\exp(E(\mathcal{A}(\mathbf{x}_i))^{\top} E(\mathcal{A}'(\mathbf{x}_i)) / \tau)}{\varepsilon' + g(\mathbf{w}; \mathbf{x}_i, \mathcal{A}, \mathcal{S}_i)}, \quad (3)$$

where  $\varepsilon' > 0$  is a small constant, which is introduced simply for the purpose of analysis to ensure the denominator that involves  $g(\mathbf{w}; \mathbf{x}_i, \mathcal{A}, \mathcal{S}_i)$  is lower bounded<sup>2</sup>, and

$$g(\mathbf{w}; \mathbf{x}_i, \mathcal{A}, \mathcal{S}_i) = \sum_{\mathbf{z} \in \mathcal{S}_i} (\exp(E(\mathcal{A}(\mathbf{x}_i))^{\top} E(\mathbf{z}) / \tau)), \quad (4)$$

which contrasts the similarity score between each positive pair  $E(\mathcal{A}(\mathbf{x}_i))^{\top} E(\mathcal{A}'(\mathbf{x}_i))$  with the similarity scores of negative pairs  $E(\mathcal{A}(\mathbf{x}_i))^{\top} E(\mathbf{z})$  for all  $\mathbf{z} \in \mathcal{S}_i$ . Based on the individual contrastive loss, we define the following **global contrastive objective (GCO)** for minimization:

$$\min_{\mathbf{w}} F(\mathbf{w}) = \mathbb{E}_{\mathbf{x}_i \sim \mathcal{D}, \mathcal{A}, \mathcal{A}' \sim \mathcal{P}} [\tau L(\mathbf{w}; \mathbf{x}_i, \mathcal{A}, \mathcal{A}')] \quad (5)$$

where  $\sim$  denotes a random sample,  $L$  is multiplied by  $\tau$  to ensure the gradient is not illy scaled. In contrast to another variant proposed in section 3.4, we refer to the above objective as the V1 GCO.

To highlight the challenge for optimizing the global contrastive objective, we consider the calculation of the gradient of  $\tau L(\mathbf{w}; \mathbf{x}_i, \mathcal{A}, \mathcal{A}')$  in terms of the parameters  $\mathbf{w}$  of the encoder network  $E$ .

$$\begin{aligned} \tau \nabla L(\mathbf{w}; \mathbf{x}_i, \mathcal{A}, \mathcal{A}') &= -\nabla(E(\mathcal{A}(\mathbf{x}_i))^{\top} E(\mathcal{A}'(\mathbf{x}_i))) \\ &+ \frac{\tau}{\varepsilon' + g(\mathbf{w}; \mathbf{x}_i, \mathcal{A}, \mathcal{S}_i)} \nabla g(\mathbf{w}; \mathbf{x}_i, \mathcal{A}, \mathcal{S}_i). \end{aligned}$$

It is notable that the first term can be easily computed by back-propogation. The challenge lies at computing the second term, where  $g(\mathbf{w}; \mathbf{x}_i, \mathcal{A}, \mathcal{S}_i)$  involves a large number of examples in  $\mathcal{S}_i$  that includes all images and their augmented data excluding that of  $\mathbf{x}_i$ . Due to the finite-sum structure of  $g$  in (4), we can compute an unbiased estimator by sampling data from  $\mathcal{S}_i$ . Indeed, we can show that  $\frac{1}{|\mathcal{B}_i|} g(\mathbf{w}; \mathbf{x}_i, \mathcal{A}, \mathcal{B}_i)$  is an unbiased estimator of  $\frac{1}{|\mathcal{S}_i|} g(\mathbf{w}; \mathbf{x}_i, \mathcal{A}, \mathcal{S}_i)$ . SimCLR directly uses

<sup>2</sup>We can also modify the definition of  $\mathcal{S}_i$  to include  $\mathcal{A}(\mathbf{x}_i)$  for ensuring  $g(\mathbf{w}; \mathbf{x}_i, \mathcal{A}, \mathcal{S}_i)$  is lower bounded without adding  $\varepsilon'$ .

this mini-batch estimator to estimate  $g(\mathbf{w}; \mathbf{x}_i, \mathcal{A}, \mathcal{S}_i)$  and  $\nabla g(\mathbf{w}; \mathbf{x}_i, \mathcal{A}, \mathcal{S}_i)$  in the above equation, yielding the following approximated gradient of  $\tau L(\mathbf{w}; \mathbf{x}_i, \mathcal{A}, \mathcal{A}')$ :

$$\begin{aligned}\tau \widehat{\nabla} L(\mathbf{x}_i, \mathcal{A}, \mathcal{A}') &= -\nabla(E(\mathcal{A}(\mathbf{x}_i))^\top E(\mathcal{A}'(\mathbf{x}_i))) \\ &\quad + \frac{\tau}{\varepsilon + g(\mathbf{w}; \mathbf{x}_i, \mathcal{A}, \mathcal{B}_i)} \nabla g(\mathbf{w}; \mathbf{x}_i, \mathcal{A}, \mathcal{B}_i),\end{aligned}\tag{6}$$

where  $\varepsilon = \frac{|\mathcal{B}_i|\varepsilon'}{|\mathcal{S}_i|}$ . However, this quantity is a biased estimator of  $\tau \nabla L(\mathbf{w}; \mathbf{x}_i, \mathcal{A}, \mathcal{A}')$  due to the non-linear function  $\frac{1}{\varepsilon + g(\mathbf{w}; \mathbf{x}_i, \mathcal{A}, \mathcal{B}_i)}$ .

### 3.2 SimCLR and its Convergence for V1 GCO

The SimCLR method can be viewed as a mini-batch based stochastic method, which uses a gradient estimator that is the average of the estimator in (6) for  $\mathbf{x}_i$  in the sampled mini-batch. To analyze the optimization error of SimCLR, we first consider the following simplest update<sup>3</sup>:

$$\mathbf{w}_{t+1} = \mathbf{w}_t - \eta \frac{1}{B} \sum_{\mathbf{x}_i \in \mathcal{B}} \widehat{\nabla} L(\mathbf{x}_i, \mathcal{A}, \mathcal{A}').\tag{7}$$

We establish the optimization error of the above update for  $T$  iterations for optimizing the V1 GCO.

**Theorem 1.** *Assume  $F$  is smooth,  $g$  is smooth and Lipchitz continuous, SimCLR with the update (7) ensures that  $\mathbb{E}[\|\nabla F(\mathbf{w}_{t'})\|^2] \leq O(\frac{1}{\eta T} + \eta + \frac{1}{B})$  for a random  $t' \in \{1, \dots, T\}$ .*

**Remark:** The above theorem implies that SimCLR suffers an optimization error at least in the order of  $O(1/\sqrt{B})$  for the objective's gradient norm. Even with  $T \rightarrow \infty$ , its optimization error is always dominated by  $O(1/\sqrt{B})$ . This explains the phenomenon that the performance of SimLCR degrades as the mini-batch size decreases. The above theorem also implies in order to find an  $\epsilon$ -level stationary solution, i.e.,  $\mathbb{E}[\|\nabla F(\mathbf{w}_t')\| \leq \epsilon]$ , we can set  $\eta = O(\epsilon^2)$  and  $T = O(1/\epsilon^4)$  and  $B = O(1/\epsilon^2)$ . All missing proofs can be found in the supplement.

### 3.3 SogCLR and its Convergence for V1 GCO

To address the issue of SimCLR, in this section we propose a memory-efficient stochastic algorithm for solving (5) without suffering from a large optimization error depending on the batch size. To this end, we decompose the objective function into three terms:

$$\begin{aligned}F(\mathbf{w}) &= \mathbb{E}_{\mathbf{x}_i \sim \mathcal{D}, \mathcal{A}, \mathcal{A}' \sim \mathcal{P}} (E(\mathcal{A}(\mathbf{x}_i))^\top E(\mathcal{A}'(\mathbf{x}_i))) \\ &\quad + \frac{\tau}{n} \sum_{\mathbf{x}_i \in \mathcal{D}} \mathbb{E}_{\mathcal{A}} \ln \left( \frac{\varepsilon'}{|\mathcal{S}_i|} + \frac{1}{|\mathcal{S}_i|} g(\mathbf{w}; \mathbf{x}_i, \mathcal{A}, \mathcal{S}_i) \right) + \text{Const},\end{aligned}\tag{8}$$

where Const is a constant that is independent of the model parameters. Below, we let  $f(\cdot) = \tau \ln(\varepsilon'/|\mathcal{S}_i| + \cdot)$ .

Our algorithm is motivated by the coupled compositional stochastic optimization studied in [27] for maximizing Average Precision, whose objective has a form of  $\frac{1}{n} \sum_i f(g_i(\mathbf{w}))$  that is similar to the second component in our objective  $F(\mathbf{w})$ . The key idea of the proposed algorithm is to keep track of  $\frac{1}{|\mathcal{S}_i|} g(\mathbf{w}; \mathbf{x}_i, \mathcal{A}, \mathcal{S}_i)$  by a scalar, whose averaged error in the long run is diminishing. However, different from the problem studied in [27], there could be many data augmentations in  $\mathcal{P}$ . As a result, by maintaining a scalar for each  $\mathbf{x}_i \in \mathcal{D}, \mathcal{A} \in \mathcal{P}$ , the memory cost is  $O(n|\mathcal{P}|)$  which increases as we increase the number of data augmentations and could be very large if  $|\mathcal{P}|$  is large. By noting that  $\mathcal{A}(\mathbf{x}_i), \forall \mathcal{A} \in \mathcal{P}$  is an augmented data from the same image for different  $\mathcal{A}$ , we expect that their embedded feature vectors are close in the sense that  $\mathbb{E}_{\mathcal{A}, \mathcal{A}', \mathbf{z}} [E(\mathcal{A}(\mathbf{x}_i))^\top E(\mathbf{z}) - E(\mathcal{A}'(\mathbf{x}_i))^\top E(\mathbf{z})]^2 \leq \epsilon^2$  for any  $\mathcal{A}, \mathcal{A}', \mathbf{x}_i$  and a small value  $\epsilon$ . By leveraging this property, we maintain and update a scalar  $\mathbf{u}_i$  for each image to track  $\frac{1}{|\mathcal{S}_i|} g(\mathbf{w}; \mathbf{x}_i, \mathcal{A}, \mathcal{S}_i)$ .

<sup>3</sup>For simplicity, we do not include another similar term in the gradient estimator by switching  $\mathcal{A}$  and  $\mathcal{A}'$ , which will not affect the analysis.

---

**Algorithm 1** SogCLR

---

- 1: **Input:**  $\mathbf{w}_0 \in \mathbb{R}^d$ , Initialize  $\mathbf{u}_0 \in \mathbb{R}^n$
- 2: Draw a batch of  $B$  samples denoted by  $\mathcal{B} = \{\mathbf{x}_i\}_{i=1}^B$ .
- 3: **for**  $t = 1, \dots, T$  **do**
- 4:   **for**  $\mathbf{x}_i \in \mathcal{B}$  **do**
- 5:     Compute  $g(\mathbf{w}_t; \mathbf{x}_i, \mathcal{A}, \mathcal{B}_i)$  and  $g(\mathbf{w}_t; \mathbf{x}_i, \mathcal{A}', \mathcal{B}_i)$  according to (2)
- 6:     Update  $\mathbf{u}_{i,t}$  according to (9)
- 7:   **end for**
- 8:   Compute the gradient estimator  $\mathbf{m}_t$  by (10)
- 9:    $\mathbf{v}_t = (1 - \beta)\mathbf{v}_{t-1} + \beta\mathbf{m}_t$
- 10:    $\mathbf{w}_{t+1} = \mathbf{w}_t - \eta\mathbf{v}_t$  (or use Adam-style update)
- 11: **end for**

---

At the  $t$ -th iteration, we update  $\mathbf{u}_i$  for  $\mathbf{x}_i \in \mathcal{B}$  by moving average

$$\begin{aligned} \mathbf{u}_{i,t} &= (1 - \gamma)\mathbf{u}_{i,t-1} \\ &+ \gamma \frac{1}{2|\mathcal{B}_i|} (g(\mathbf{w}_t; \mathbf{x}_i, \mathcal{A}, \mathcal{B}_i) + g(\mathbf{w}_t; \mathbf{x}_i, \mathcal{A}', \mathcal{B}_i)), \end{aligned} \quad (9)$$

where  $\gamma \in (0, 1)$ . Then we can compute a stochastic gradient estimator by

$$\begin{aligned} \mathbf{m}_t &= -\frac{1}{B} \sum_{\mathbf{x}_i \in \mathcal{B}} \nabla(E(\mathcal{A}(\mathbf{x}_i))^\top E(\mathcal{A}'(\mathbf{x}_i))) \\ &+ \frac{p_{i,t}}{2|\mathcal{B}_i|} (\nabla g(\mathbf{w}_t; \mathbf{x}_i, \mathcal{A}, \mathcal{B}_i) + \nabla g(\mathbf{w}_t; \mathbf{x}_i, \mathcal{A}', \mathcal{B}_i)). \end{aligned} \quad (10)$$

where  $p_{i,t} = \frac{\tau}{\varepsilon'/|\mathcal{S}_i| + u_{i,t-1}} = \nabla f(u_{i,t-1})$ . Finally, we can update the model parameter  $\mathbf{w}_{t+1}$  by using a momentum-style update or an Adam-style update. The detailed steps are summarized in Algorithm 1, which is referred as SogCLR to emphasize that we aim to optimize the global contrastive objective.

We note that the memory cost of SogCLR is  $O(n + d)$ , which is  $O(d)$  for over-parameterized deep neural networks with  $d \gg n$ . The per-iteration complexity of SogCLR is the same as SimCLR.

Next, we provide a convergence result for SogCLR.

**Theorem 2.** Assume that  $\mathbb{E}_{\mathcal{A}, \mathcal{A}'} \mathbb{E}_{\mathbf{z} \sim \mathcal{S}_i} |E(\mathcal{A}(\mathbf{x}_i))^\top E(\mathbf{z}) - E(\mathcal{A}'(\mathbf{x}_i))^\top E(\mathbf{z})|^2 \leq \epsilon^2$  for any  $\mathbf{x}_i \in \mathcal{D}$  and the same conditions as in Theorem 1 hold, then with  $\gamma \leq \frac{n}{B}$ , and  $\eta = O(\min\{\beta, \frac{\gamma B}{n}, \frac{1}{L_F}\})$ , after  $T$  iterations, SogCLR ensures that  $\mathbb{E}[\|\nabla F(\mathbf{w}_{t'})\|^2] \leq O(\frac{1}{\eta T} + \frac{\beta + \gamma}{B} + \epsilon^2)$  for a random  $t' \in \{1, \dots, T\}$ .

**Remark:** The above theorem implies that by setting  $\beta = \sqrt{B/T} < 1$  and  $\gamma = \sqrt{n/T} < 1$ , then SogCLR's optimization error will converge to the level of  $\epsilon$  when  $T = O(\max(\frac{n}{B^2\epsilon^4}, \frac{1}{B\epsilon^4}))$ , i.e.,  $\mathbb{E}[\|\nabla F(\mathbf{w}_{t'})\|^2] \leq O(\frac{1}{\sqrt{BT}} + \frac{\sqrt{n}}{B\sqrt{T}} + \epsilon^2) \leq O(\epsilon^2)$ . When  $\epsilon$  is small enough, the optimization error of SogCLR is negligible. In addition, the analysis also implies that SogCLR enjoys a parallel speed-up, i.e., with a larger mini-batch size  $B$  it needs a less number of iterations to converge to a small error.

One might notice that there are two differences between SogCLR and the update (7) for SimCLR. One difference is that SogCLR maintains and updates the  $\mathbf{u}$  sequence. The second difference is that SogCLR uses a momentum-style update. We would like to emphasize that the moving average update for  $\mathbf{u}_{i,t+1}$  is the key to prove the above result. With this technique, SogCLR is able to leverage the momentum-style update or the Adam-style update to enjoy a small optimization error. Without using the scalars  $\mathbf{u}_{i,t+1}$  in computing the gradient estimator, even we use the momentum-style update or the Adam-style update for SimCLR, it still suffers from an optimization error in the order of  $O(1/\sqrt{B})$ . In particular, we have the following corollary for the optimization error of SimCLR with the momentum-style update.

**Corollary 1.** Let us consider the following momentum-style update for SimCLR.

$$\mathbf{v}_t = (1 - \beta)\mathbf{v}_{t-1} + \beta \frac{\tau}{B} \sum_{\mathbf{x}_i \in \mathcal{B}} \hat{\nabla} L(\mathbf{x}_i, \mathcal{A}, \mathcal{A}') \quad (11)$$

$$\mathbf{w}_{t+1} = \mathbf{w}_t - \eta \mathbf{v}_t. \quad (12)$$

Assume  $F$  is smooth,  $g$  is smooth and Lipschitz continuous, with  $\eta \leq O(\beta)$  SimCLR ensures that  $\mathbb{E}[\|\nabla F(\mathbf{w}_{t'})\|^2] \leq O(\frac{1}{\eta T} + \frac{1}{\beta T} + \frac{\beta}{B} + \frac{1}{B})$  for a random  $t' \in \{1, \dots, T\}$ .

**Remark:** The dominating term in the upper bound is still  $O(1/B)$  when  $T \rightarrow \infty$  and  $\beta = O(1/\sqrt{T})$ .

### 3.4 SogCLR optimizes V2 Global Contrastive Objective

In this section, we propose another version of the global contrastive objective (V2) and show that SogCLR optimizes the V2 global contrastive objective, which further justifies the proposed algorithm SogCLR. In particular, let us consider the following objective.

$$\begin{aligned} F_{v2}(\mathbf{w}) &= \mathbb{E}_{\mathbf{x}_i \sim \mathcal{D}, \mathcal{A}, \mathcal{A}' \sim \mathcal{P}} (E(\mathcal{A}(\mathbf{x}_i))^\top E(\mathcal{A}'(\mathbf{x}_i))) \\ &+ \frac{1}{n} \sum_{\mathbf{x}_i \in \mathcal{D}} \ln \left( \frac{\varepsilon'}{|\mathcal{S}_i|} + \frac{\tau}{|\mathcal{S}_i|} \mathbb{E}_{\mathcal{A}g}(\mathbf{w}; \mathbf{x}_i, \mathcal{A}, \mathcal{S}_i) \right) + \text{Const.} \end{aligned} \quad (13)$$

The difference between V2 GCO (13) and V1 GCO (5) is that the expectation over  $\mathcal{A}$  in the second component is moved from the outside the logarithmic function to the inside. The above objective function can be also explained from the average of individual contrastive loss. To this end, we define the following contrastive loss for each augmented pair  $(\mathcal{A}(\mathbf{x}_i), \mathcal{A}'(\mathbf{x}_i))$ :

$$L_2(\mathbf{w}; \mathbf{x}_i, \mathcal{A}, \mathcal{A}') = -\ln \frac{\exp(E(\mathcal{A}(\mathbf{x}_i))^\top E(\mathcal{A}'(\mathbf{x}_i))/\tau)}{\varepsilon' + \mathbb{E}_{\mathcal{A}g}(\mathbf{w}; \mathbf{x}_i, \mathcal{A}, \mathcal{S}_i)}. \quad (14)$$

Then we have

$$F_{v2}(\mathbf{w}) = \mathbb{E}_{\mathbf{x} \sim \mathcal{D}, \mathcal{A}, \mathcal{A}'} [\tau L_2(\mathbf{w}; \mathbf{x}_i, \mathcal{A}, \mathcal{A}')].$$

Different from  $L(\mathbf{w}; \mathbf{x}_i, \mathcal{A}, \mathcal{A}')$ , in the definition of  $L_2(\mathbf{w}; \mathbf{x}_i, \mathcal{A}, \mathcal{A}')$  the similarity score of a positive pair  $(\mathcal{A}(\mathbf{x}_i), \mathcal{A}'(\mathbf{x}_i))$  is contrasted with all possible negative pairs between  $\mathbf{x}_i$  and other images.

We prove that SogCLR indeed converges to a stationary solution to the V2 GCO  $F_{v2}(\mathbf{w})$ . Different from  $F(\mathbf{w})$  defined in (5), the update of  $u$  of SogCLR can be considered directly as a moving average estimator of  $\mathbb{E}_{\mathcal{A}g}(\mathbf{w}; \mathbf{x}_i, \mathcal{A}, \mathcal{S}_i)$  in  $F_{v2}(\mathbf{w})$ , which does not involve the error caused by difference between different augmented data. We state the convergence below.

**Theorem 3.** Assume the same conditions as in Theorem 1 hold, then with  $\gamma \leq \frac{n}{B}$ , and  $\eta = O(\min \left\{ \beta, \frac{\gamma B}{n}, \frac{1}{L_F} \right\})$ , after  $T$  iterations, SogCLR ensures that  $\mathbb{E}[\|\nabla F_{v2}(\mathbf{w}_{t'})\|^2] \leq O(\frac{1}{\eta T} + \frac{\beta + \gamma}{B})$  for a random  $t' \in \{1, \dots, T\}$ .

**Remark:** The above theorem implies that by setting  $\beta = \sqrt{B/T} < 1$  and  $\gamma = \sqrt{n/T} < 1$ , then SogCLR converges to a stationary solution of  $F_{v2}(\mathbf{w})$  when  $T \rightarrow \infty$ .

## 4 Extensions

In this section, we propose the extension of the proposed technique for optimizing other contrastive losses. We note that the large batch size requirement also exists in other contrastive learning methods. Below we consider one task, namely a self-supervised bimodal contrastive learning task.

**Optimizing Two-way Contrastive Objective.** A recent paper [29] proposes a bimodal contrastive learning method named CLIP, which uses a two-way contrastive loss to learn both the encoder network for the image and the encoder network for the text. [29] use a very large batch size 32,768 on a self-collected large-scale dataset with 400 millions image and text pairs. Inspired by the SogCLR method for optimizing one-way contrastive loss and its promising performance, below we present a similar solution to alleviate the requirement of large batch size for optimizing two-way contrastive

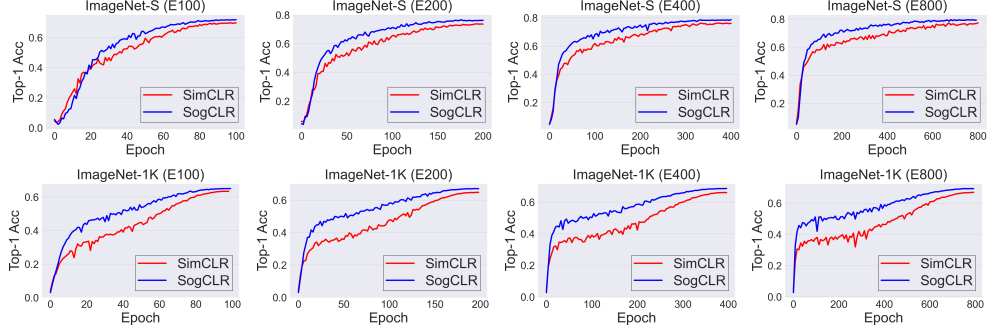


Figure 1: Learning curve for top-1 accuracy by linear evaluation on ImageNet-S and ImageNet-1K trained on R50 with batch size of 256.

loss. Given a set of image-text pairs  $\mathcal{D} = \{(\mathbf{x}_1, \mathbf{t}_1), \dots, (\mathbf{x}_n, \mathbf{t}_n)\}$ . We denote by  $E_I$  and  $E_T$  the encoder network for the image data and the text data, respectively. We can consider optimizing a global two-way contrastive loss:

$$F(\mathbf{w}) = -\frac{\tau}{n} \sum_{i=1}^n \log \frac{\exp(E_I(\mathbf{x}_i)^\top E_T(\mathbf{t}_i)/\tau)}{\sum_{\mathbf{t} \in \mathcal{D}} \exp(E_I(\mathbf{x}_i)^\top E_T(\mathbf{t})/\tau)} - \frac{\tau}{n} \sum_{i=1}^n \log \frac{\exp(E_I(\mathbf{x}_i)^\top E_T(\mathbf{t}_i)/\tau)}{\sum_{\mathbf{x} \in \mathcal{D}} \exp(E_I(\mathbf{x})^\top E_T(\mathbf{t}_i)/\tau)}.$$

Due to the large size of  $\mathcal{D}$ , the challenge lies that handling  $g(\mathbf{w}; \mathbf{x}_i) = \mathbb{E}_{\mathbf{t} \sim \mathcal{D}} \exp(E_I(\mathbf{x}_i)^\top E_T(\mathbf{t})/\tau)$  and  $g(\mathbf{w}; \mathbf{t}_i) = \mathbb{E}_{\mathbf{x} \sim \mathcal{D}} \exp(E_I(\mathbf{x})^\top E_T(\mathbf{t}_i)/\tau)$ . We propose to compute a stochastic gradient estimator by

$$\begin{aligned} \mathbf{m}_t = & -\frac{1}{B} \sum_{i \in \mathcal{B}} E_I(\mathbf{x}_i)^\top E_T(\mathbf{t}_i) + \\ & \frac{1}{B} \sum_{i \in \mathcal{B}} \left( \frac{\tau}{u_{i,t}^I} \nabla g(\mathbf{w}_t; \mathbf{x}_i, \mathcal{B}) + \frac{\tau}{u_{i,t}^T} \nabla g(\mathbf{w}_t; \mathbf{t}_i, \mathcal{B}) \right) \end{aligned}$$

where  $g(\mathbf{w}; \mathbf{x}_i, \mathcal{B})$  and  $g(\mathbf{w}; \mathbf{t}_i, \mathcal{B})$  are the mini-batch estimators of  $g(\mathbf{w}; \mathbf{x}_i)$  and  $g(\mathbf{w}; \mathbf{t}_i)$  respectively. The scalar  $u_{i,t+1}^I$  and  $u_{i,t+1}^T$  are updated for the sampled data according to

$$\begin{aligned} u_{i,t+1}^I &= (1 - \gamma) u_{i,t}^I + \gamma g(\mathbf{w}_t; \mathbf{x}_i, \mathcal{B}) \\ u_{i,t+1}^T &= (1 - \gamma) u_{i,t}^T + \gamma g(\mathbf{w}_t; \mathbf{t}_i, \mathcal{B}). \end{aligned}$$

Then we can update the model by Adam-style update or momentum-style update.

## 5 Experiments

In this section, we compare SogCLR to SimCLR to demonstrate the effectiveness of our optimization method. For a fair comparison, we adopt the same settings as SimCLR to SogCLR unless noted (main difference is the batch size). It is not our focus to leverage multiple techniques for achieving state-of-the-art performance [31]. We also compare with the CLIP framework for bimodal contrastive learning. We aim to demonstrate SogCLR can achieve competitive performance when using a smaller batch size. For SimCLR, we run experiments on two scales of ImageNet dataset. The small version is a subset with randomly selected 100 classes (about 128k images) from ImageNet denoted as ImageNet-S [33], and the full version of ImageNet (about 1.2 million images) is denoted as ImageNet-1K [8]. For CLIP, we manually construct a text-image pair dataset based on ImageNet-S using the label of each image to construct a text. For the implementations, we follow these open-source repositories [2, 29, 18] available in Github. All experiments related to SimCLR are trained on Google Cloud TPUs using 8 to 512 cores depending on model size and batch size. All experiments related to CLIP are trained a NVIDIA V100 GPU with 32GB memory size.

## 5.1 Image Pretraining

**Experiment setup.** Following previous works [2, 3], we pretrain ResNet-50 [17] with a 2-layer  $128 \times 128$  MLP projection head on top of backbone encoder. We explore different batch sizes of 128, 256, 512 and different training epochs of 100, 200, 400, 800. We use square root learning rate scaling ( $0.075 \times \sqrt{\text{BatchSize}}$ ) with a cosine decay schedule without restart. We also use learning rate warm-up for 10 epochs, i.e., learning rate is gradually increased to maximum value. We follow the same image augmentation strategies as in SimCLR [2, 3] including random crop, color distortion, and Gaussian blur. We use LARS optimizer [34] (with a momentum of 0.9 and weight decay of 1e-6) and set temperature( $\tau$ ) to 0.1 by default for all pretraining experiments. For SogCLR in Algorithm 1, we tune  $\gamma$  in [0.99, 0.9, 0.8, 0.7, 0.6] and initialize sequence  $\mathbf{u}_0$  by all zeros. For evaluations, we report performance for linear classifier trained on top of the pretrained encoder on ImageNet validation sets known as linear evaluation [2, 16, 1, 12]. In particular, we train a linear classifier using SGD with Nesterov momentum with a batch size of 4096 and learning rate of 0.1 for 90 epochs. For training, We random crop and resize input images to  $224 \times 224$ . For testing, we apply center crop on input images.

**Results.** We report top-1 accuracy by linear evaluation on ImageNet-S and ImageNet-1K under different batch sizes and training epochs in Table 1 and Table 2. We can see that SogCLR performs consistently better than SimCLR under all settings on two datasets. SogCLR achieves 3.9%, 2.3%, 1.9% average improvements on ImageNet-S and achieves 2.8%, 2.3%, 1.3% average improvements on ImageNet-1K with batch size of 128, 256, 512, respectively. In particular, we achieve 69.4% top-1 accuracy using only batch size of 256, which is better than original SimCLR’s large-batch (e.g., 4096, 8192) results at 69.1% under the same number of epochs. In addition, we compare the convergence speed of SogCLR with SimCLR using the same batch size of 256 with different number of epochs on ImageNet-S and ImageNet-1K as shown in Figure 1. The results indicate that our algorithm converges faster in terms of number of epochs using small batch sizes.

Table 1: Linear evaluation (top-1 accuracy) under different batch sizes and training epoch on ResNet-50 and ImageNet-S.

| Method | BatchSize\Epoch | 100         | 200         | 400         | 800         |
|--------|-----------------|-------------|-------------|-------------|-------------|
| SimCLR | 128             | 68.5        | 72.7        | 75.7        | 75.7        |
| SogCLR | 128             | <b>72.2</b> | <b>76.7</b> | <b>79.3</b> | <b>80.1</b> |
| SimCLR | 256             | 69.7        | 73.6        | 76.1        | 77.4        |
| SogCLR | 256             | <b>71.8</b> | <b>76.3</b> | <b>78.7</b> | <b>79.4</b> |
| SimCLR | 512             | 70.9        | 74.1        | 75.9        | 76.3        |
| SogCLR | 512             | <b>71.8</b> | <b>75.8</b> | <b>78.2</b> | <b>79.4</b> |

Table 2: Linear evaluation (top-1 accuracy) under different batch sizes and training epoch on ResNet-50 and ImageNet-1K.

| Method | BatchSize\Epoch | 100         | 200         | 400         | 800         |
|--------|-----------------|-------------|-------------|-------------|-------------|
| SimCLR | 128             | 62.6        | 64.0        | 64.1        | 64.5        |
| SogCLR | 128             | <b>64.9</b> | <b>66.2</b> | <b>67.4</b> | <b>67.9</b> |
| SimCLR | 256             | 62.8        | 64.3        | 65.7        | 66.5        |
| SogCLR | 256             | <b>65.2</b> | <b>67.1</b> | <b>68.7</b> | <b>69.4</b> |
| SimCLR | 512             | 63.8        | 65.6        | 66.7        | 67.4        |
| SogCLR | 512             | <b>65.0</b> | <b>67.2</b> | <b>68.8</b> | <b>69.6</b> |

## 5.2 Vision and Language Pretraining

**Experiment Setup.** In this section, we aims to demonstrate our algorithm can also be applied to solve bi-modal self-supervised problems. We study a popular vision and language pretraining framework, i.e., CLIP [29]. CLIP consists of two parts: vision encoder (e.g., CNN, transformer) and text encoder (e.g., transformer). The original CLIP is pretrained on a large dataset with 400 million image-text pairs to achieve the competitive performance against supervised baseline. Here, we are not aiming to achieve the best performance but to study and understand the limits of this framework. Thus, we use the modified CLIP consisting of a modified ResNet-50 and a small vision

transformer(ViT) [11], denoted as CLIP-S. The detailed configuration can be found in Appendix. We use template "*This is a photo of [CLASS]*" to generate the text caption for each image based on ImageNet-S. For training, we use batch size of 128 and 256 to train the models for 30 and 60 epochs. We use warm-up strategy for 1000 iterations to increase learning rate to the maximum value of 0.001 and then decrease it by a cosine decay scheduler. We use Adam-W optimizer [23] with the weight decay of 0.1. We set temperature to a fixed value for 0.07 for SogCLR and CLIP. Similar to SimCLR, we tune  $\gamma = [0.6 \sim 0.99]$  and set  $\mathbf{u}_0$  to zeros for SogCLR. For evaluations, we perform zero-shot evaluation on ImageNet-S validation set using the ensemble results of 80 different prompt templates [29]. The validation results are presented in Table 3.

**Results.** We report zero-shot evaluation accuracy of CLIP-S in Table 3. The results indicate that CLIP-S trained by SogCLR performs better than CLIP-S trained by standard InfoNCE loss. In addition, we observe that InfoNCE suffers from 4% performance drop for training 60 epochs. In contrast, SogCLR has much stable performance for longer training and achieves over 1% improvement on zero-shot evaluation accuracy. In addition, we also find that CLIP with SogCLR is much robust to the change of batch size while CLIP with InfoNCE drops more than 1% when switching batch size from 256 to 128.

Table 3: Top-1 evaluation accuracy under different batch sizes for bimodal learning on ImageNet-S.

| Method\BatchSize | Epoch       |             | 30          | 60          |
|------------------|-------------|-------------|-------------|-------------|
|                  | 128         | 256         | 128         | 256         |
| CLIP-S+InfoNCE   | 67.7        | 69.0        | 63.4        | 64.9        |
| CLIP-S+SogCLR    | <b>69.5</b> | <b>69.4</b> | <b>71.3</b> | <b>70.1</b> |

### 5.3 Ablation Studies

**Verification of algorithmic design and theory.** We validate (i) using the momentum update for  $u_{t+1}$  (i.e.,  $\gamma < 1$ ) is better than without using momentum update ( $\gamma = 1$ ). (ii)  $\mathbb{E}_{\mathcal{A}, \mathcal{A}', \mathbf{z}}[|E(\mathcal{A}(\mathbf{x}_i))^\top E(\mathbf{z}) - E(\mathcal{A}'(\mathbf{x}_i))^\top E(\mathbf{z})|^2] \leq \epsilon^2$  in Theorem 2 holds with a small  $\epsilon^2$ . In other words, we expect the similarity between the representations of different augmented samples are close. For (i), we train ResNet-50 with batch size of 256 for 100, 200, 400, 800 epochs. We tune the  $\gamma$  in [0.6, 0.7, 0.8, 0.9, 0.99]. The results are summarized in the Table 7 in Appendix. The results indicate that models with  $\gamma = 0.7 \sim 0.8$  achieve the best performance. For (ii), we use the models trained with batch size 256 at the checkpoints of 100th, 200th, 400th, 800th epoch to compute  $\mathbb{E}_{\mathcal{A}, \mathcal{A}', \mathbf{z}}[|\mathcal{A}(\mathbf{x}_i)^\top \mathbf{z} - \mathcal{A}'(\mathbf{x}_i)^\top \mathbf{z}|^2]$  on ImageNet-S, where the expectation is approximated by the Monte Carlo method. We show the histograms of this quantity for all images  $\mathbf{x}_i$  in Figure 2, which suggests that all data samples satisfy the above condition in Theorem 2 for some small  $\epsilon$ .

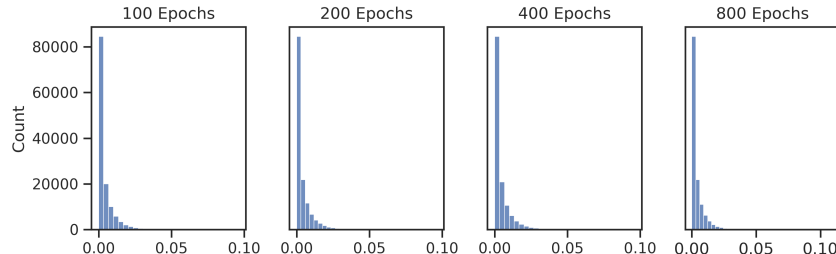


Figure 2: Histogram for difference of learned features between different augmented samples. X-axis is the value for  $\mathbb{E}_{\mathcal{A}, \mathcal{A}', \mathbf{z}}[|E(\mathcal{A}(\mathbf{x}_i))^\top E(\mathbf{z}) - E(\mathcal{A}'(\mathbf{x}_i))^\top E(\mathbf{z})|^2]$  and Y-axis denotes the count number.

**Impact of batch size.** Since SimCLR suffers from the performance drop due to small batch sizes. Here, we show SogCLR is robust to smaller batch sizes. To verify this hypothesis, we train SogCLR using batch sizes varying from 128 to 8192 with ResNet-50 on ImageNet-1K. We set a fixed  $\gamma = 0.8$ . We directly compare the results taken from Table B.1 in [2] using same settings. As shown in Figure 3, the performance of SimCLR drops quickly as the decrease of batch size. As a comparison, SogCLR remains stable with batch size from 8192 to 256 and there is a small drop on batch size 128. Overall,

SogCLR demonstrates the robustness to different batch sizes. This result is consistent with our theory.

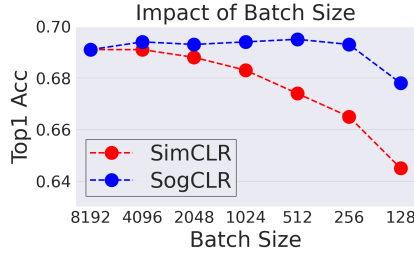


Figure 3: Impact of batch size. Y-axis is linear evaluation accuracy with 800-epoch pretraining with ResNet-50 on ImageNet-1K.

**Different network encoders.** To verify the effectiveness of proposed method, we further evaluate it on different network encoders. To this end, we train ResNet models by varying width. We train ResNet-50 ( $2\times, 4\times$ ) using batch size of 512 for 800 epochs. We set  $\gamma = 0.8$ . For baselines, we use the batch size of 4096 to train models for a total of 1000 epochs. The results are summarized in the table below. When using ResNet-50 ( $2\times, 4\times$ ), we are able to achieve 74.6% and 76.7% Top-1 linear evaluation accuracy, which are better than SimCLR’s results trained with a larger batch size of 4096 and a large epoch number.

Table 4: Performance with ResNet-50 ( $2\times, 4\times$ ) on ImageNet-1K.

| Method | Encoder           | Params | BatchSize | Top1        | Top5 |
|--------|-------------------|--------|-----------|-------------|------|
| SimCLR | R50 ( $2\times$ ) | 94M    | 4096      | 74.2        | 92.0 |
| SogCLR | R50 ( $2\times$ ) | 94M    | 512       | <b>74.6</b> | 92.1 |
| SimCLR | R50 ( $4\times$ ) | 375M   | 4096      | 76.5        | 93.2 |
| SogCLR | R50 ( $4\times$ ) | 375M   | 512       | <b>76.7</b> | 93.1 |

**Effects of projection heads.** The nonlinear projection head is essential for SimCLR to learn high-quality representations [2]. To verify the impact of different projection heads, we adopt a 3-layer MLP projection head ( $128 \times 128 \times 128$ ) on the top of ResNet-50 encoder and repeat the same experiments in section 5.1 by pretraining the models with batch sizes of 256, 512 and epochs of 100, 200, 400, 800. The temperature  $\tau$  is fixed to 0.1. The results are summarized in the following table. By the comparison of Table 5 and Table 2, we can see that both SimCLR and SogCLR improve more than 1% Top-1 linear accuracy. In particular, SogCLR achieves the highest Top-1 linear accuracy 71.2% without using memory bank mechanism, which is better than 71.1% achieved by MoCo-v2 [4].

Table 5: Linear evaluation (top-1 accuracy) for using a 3-layer MLP projection head under different batch sizes and training epoch on ResNet-50 and ImageNet-1k.

| Method | BatchSize\Epoch | 100         | 200         | 400         | 800         |
|--------|-----------------|-------------|-------------|-------------|-------------|
| SimCLR | 256             | 63.9        | 65.3        | 66.7        | 67.5        |
| SogCLR | 256             | <b>66.7</b> | <b>68.7</b> | <b>70.1</b> | <b>70.7</b> |
| SimCLR | 512             | 65.1        | 66.7        | 67.6        | 68.7        |
| SogCLR | 512             | <b>66.6</b> | <b>68.7</b> | <b>70.1</b> | <b>71.2</b> |

## 6 Conclusion

In this paper, we have examined the large batch size issue in the training of contrastive self-supervised learning from an optimization perspective. To address this issue, we have proposed a global contrastive objective and an efficient stochastic algorithm with provable convergence guarantee. Our analysis also exhibits why existing methods such as SimCLR require a large batch size for ensuring the optimization error to be small. For future work, we plan to incorporate more advanced techniques into the proposed method to further improve the performance.

## Acknowledgements

We would like to thank Quanqi Hu for help on the proofs.

## References

- [1] Mathilde Caron, Ishan Misra, Julien Mairal, Priya Goyal, Piotr Bojanowski, and Armand Joulin. Unsupervised learning of visual features by contrasting cluster assignments. *arXiv preprint arXiv:2006.09882*, 2020.
- [2] Ting Chen, Simon Kornblith, Mohammad Norouzi, and Geoffrey Hinton. A simple framework for contrastive learning of visual representations. In *International conference on machine learning*, pages 1597–1607. PMLR, 2020.
- [3] Ting Chen, Simon Kornblith, Kevin Swersky, Mohammad Norouzi, and Geoffrey Hinton. Big self-supervised models are strong semi-supervised learners. *arXiv preprint arXiv:2006.10029*, 2020.
- [4] Xinlei Chen, Haoqi Fan, Ross Girshick, and Kaiming He. Improved baselines with momentum contrastive learning. *arXiv preprint arXiv:2003.04297*, 2020.
- [5] Xinlei Chen, Saining Xie, and Kaiming He. An empirical study of training self-supervised vision transformers. *arXiv preprint arXiv:2104.02057*, 2021.
- [6] Sumit Chopra, Raia Hadsell, and Yann LeCun. Learning a similarity metric discriminatively, with application to face verification. In *2005 IEEE Computer Society Conference on Computer Vision and Pattern Recognition (CVPR’05)*, volume 1, pages 539–546. IEEE, 2005.
- [7] Cong D Dang and Guanghui Lan. Stochastic block mirror descent methods for nonsmooth and stochastic optimization. *SIAM Journal on Optimization*, 25(2):856–881, 2015.
- [8] Jia Deng, Wei Dong, Richard Socher, Li-Jia Li, Kai Li, and Li Fei-Fei. Imagenet: A large-scale hierarchical image database. In *2009 IEEE conference on computer vision and pattern recognition*, pages 248–255. Ieee, 2009.
- [9] Jacob Devlin, Ming-Wei Chang, Kenton Lee, and Kristina Toutanova. Bert: Pre-training of deep bidirectional transformers for language understanding. *arXiv preprint arXiv:1810.04805*, 2018.
- [10] Alexey Dosovitskiy, Lucas Beyer, Alexander Kolesnikov, Dirk Weissenborn, Xiaohua Zhai, Thomas Unterthiner, Mostafa Dehghani, Matthias Minderer, Georg Heigold, Sylvain Gelly, et al. An image is worth 16x16 words: Transformers for image recognition at scale. *arXiv preprint arXiv:2010.11929*, 2020.
- [11] Alexey Dosovitskiy, Lucas Beyer, Alexander Kolesnikov, Dirk Weissenborn, Xiaohua Zhai, Thomas Unterthiner, Mostafa Dehghani, Matthias Minderer, Georg Heigold, Sylvain Gelly, Jakob Uszkoreit, and Neil Houlsby. An image is worth 16x16 words: Transformers for image recognition at scale. *ArXiv*, abs/2010.11929, 2021.
- [12] Jean-Bastien Grill, Florian Strub, Florent Altché, Corentin Tallec, Pierre H Richemond, Elena Buchatskaya, Carl Doersch, Bernardo Avila Pires, Zhaohan Daniel Guo, Mohammad Gheshlaghi Azar, et al. Bootstrap your own latent: A new approach to self-supervised learning. *arXiv preprint arXiv:2006.07733*, 2020.
- [13] Zhishuai Guo, Yi Xu, Wotao Yin, Rong Jin, and Tianbao Yang. On stochastic moving-average estimators for non-convex optimization. *arXiv preprint arXiv:2104.14840*, 2021.
- [14] Michael Gutmann and Aapo Hyvärinen. Noise-contrastive estimation: A new estimation principle for unnormalized statistical models. In *Proceedings of the thirteenth international conference on artificial intelligence and statistics*, pages 297–304. JMLR Workshop and Conference Proceedings, 2010.
- [15] Raia Hadsell, Sumit Chopra, and Yann LeCun. Dimensionality reduction by learning an invariant mapping. In *2006 IEEE Computer Society Conference on Computer Vision and Pattern Recognition (CVPR’06)*, volume 2, pages 1735–1742. IEEE, 2006.
- [16] Kaiming He, Haoqi Fan, Yuxin Wu, Saining Xie, and Ross Girshick. Momentum contrast for unsupervised visual representation learning. In *Proceedings of the IEEE/CVF Conference on Computer Vision and Pattern Recognition*, pages 9729–9738, 2020.

- [17] Kaiming He, Xiangyu Zhang, Shaoqing Ren, and Jian Sun. Deep residual learning for image recognition. In *Proceedings of the IEEE conference on computer vision and pattern recognition*, pages 770–778, 2016.
- [18] Gabriel Ilharco, Mitchell Wortsman, Nicholas Carlini, Rohan Taori, Achal Dave, Vaishaal Shankar, Hongseok Namkoong, John Miller, Hannaneh Hajishirzi, Ali Farhadi, and Ludwig Schmidt. Openclip. *Zenodo*, 2021.
- [19] Prannay Khosla, Piotr Teterwak, Chen Wang, Aaron Sarna, Yonglong Tian, Phillip Isola, Aaron Maschinot, Ce Liu, and Dilip Krishnan. Supervised contrastive learning. *arXiv preprint arXiv:2004.11362*, 2020.
- [20] Zhenzhong Lan, Mingda Chen, Sebastian Goodman, Kevin Gimpel, Piyush Sharma, and Radu Soricut. Albert: A lite bert for self-supervised learning of language representations. *arXiv preprint arXiv:1909.11942*, 2019.
- [21] Chunyuan Li, Jianwei Yang, Pengchuan Zhang, Mei Gao, Bin Xiao, Xiyang Dai, Lu Yuan, and Jianfeng Gao. Efficient self-supervised vision transformers for representation learning. *arXiv preprint arXiv:2106.09785*, 2021.
- [22] Ze Liu, Yutong Lin, Yue Cao, Han Hu, Yixuan Wei, Zheng Zhang, Stephen Lin, and Baining Guo. Swin transformer: Hierarchical vision transformer using shifted windows. *arXiv preprint arXiv:2103.14030*, 2021.
- [23] Ilya Loshchilov and Frank Hutter. Decoupled weight decay regularization. *arXiv preprint arXiv:1711.05101*, 2017.
- [24] Tomas Mikolov, Kai Chen, Greg Corrado, and Jeffrey Dean. Efficient estimation of word representations in vector space. *arXiv preprint arXiv:1301.3781*, 2013.
- [25] Jovana Mitrovic, Brian McWilliams, Jacob Walker, Lars Buesing, and Charles Blundell. Representation learning via invariant causal mechanisms. *arXiv preprint arXiv:2010.07922*, 2020.
- [26] Aaron van den Oord, Yazhe Li, and Oriol Vinyals. Representation learning with contrastive predictive coding. *arXiv preprint arXiv:1807.03748*, 2018.
- [27] Qi Qi, Youzhi Luo, Zhao Xu, Shuiwang Ji, and Tianbao Yang. Stochastic optimization of areas under precision-recall curves with provable convergence. *Advances in Neural Information Processing Systems*, 34, 2021.
- [28] Rui Qian, Tianjian Meng, Boqing Gong, Ming-Hsuan Yang, H. Wang, Serge J. Belongie, and Yin Cui. Spatiotemporal contrastive video representation learning. *2021 IEEE/CVF Conference on Computer Vision and Pattern Recognition (CVPR)*, pages 6960–6970, 2021.
- [29] Alec Radford, Jong Wook Kim, Chris Hallacy, Aditya Ramesh, Gabriel Goh, Sandhini Agarwal, Girish Sastry, Amanda Askell, Pamela Mishkin, Jack Clark, et al. Learning transferable visual models from natural language supervision. *arXiv preprint arXiv:2103.00020*, 2021.
- [30] Kihyuk Sohn. Improved deep metric learning with multi-class n-pair loss objective. In *Advances in neural information processing systems*, pages 1857–1865, 2016.
- [31] Nenad Tomasev, Ioana Bica, Brian McWilliams, Lars Buesing, Razvan Pascanu, Charles Blundell, and Jovana Mitrovic. Pushing the limits of self-supervised resnets: Can we outperform supervised learning without labels on imagenet? *arXiv preprint arXiv:2201.05119*, 2022.
- [32] Bokun Wang and Tianbao Yang. Finite-sum coupled compositional stochastic optimization: theories and applications. *CoRR*, 2022.
- [33] Yue Wu, Yinpeng Chen, Lijuan Wang, Yuancheng Ye, Zicheng Liu, Yandong Guo, and Yun Fu. Large scale incremental learning. In *Proceedings of the IEEE/CVF Conference on Computer Vision and Pattern Recognition*, pages 374–382, 2019.
- [34] Yang You, Igor Gitman, and Boris Ginsburg. Large batch training of convolutional networks. *arXiv preprint arXiv:1708.03888*, 2017.
- [35] Jure Zbontar, Li Jing, Ishan Misra, Yann LeCun, and Stéphane Deny. Barlow twins: Self-supervised learning via redundancy reduction. In *International Conference on Machine Learning*, pages 12310–12320. PMLR, 2021.
- [36] Xiaohua Zhai, Alexander Kolesnikov, Neil Houlsby, and Lucas Beyer. Scaling vision transformers. *ArXiv*, abs/2106.04560, 2021.

- [37] Yuhao Zhang, Hang Jiang, Yasuhide Miura, Christopher D Manning, and Curtis Langlotz. Contrastive learning of medical visual representations from paired images and text, 2021.
- [38] Xizhou Zhu, Weijie Su, Lewei Lu, Bin Li, Xiaogang Wang, and Jifeng Dai. Deformable detr: Deformable transformers for end-to-end object detection. *arXiv preprint arXiv:2010.04159*, 2020.

## A Experiment Details

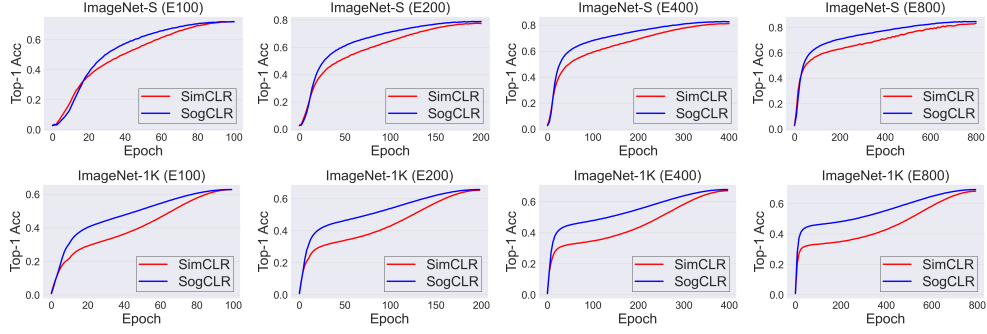


Figure 4: Learning curve for top-1 accuracy by linear evaluation on ImageNet-S and ImageNet-1K training set trained on ResNet-50 using batch size of 256.

Table 6: CLIP-S hyper-parameters.

| Hyperparameter     | Value     |
|--------------------|-----------|
| embed_dim          | 512       |
| image_resolution   | 224×224   |
| vision_layers      | [3,4,6,3] |
| vision_width       | 32        |
| vision_patch_size  | null      |
| context_length     | 77        |
| vocab_size         | 49408     |
| transformer_width  | 128       |
| transformer_heads  | 8         |
| transformer_layers | 8         |

Table 7: Top-1 linear evaluation accuracy trained on ResNet-50 under different number of epochs using batch size of 256 on ImageNet-1K for  $\gamma = 1$  v.s.  $\gamma < 1$  in Algorithm 1.

| $\gamma \backslash \text{Epoch}$ | 100         | 200         | 400         | 800         |
|----------------------------------|-------------|-------------|-------------|-------------|
| 1.0                              | 62.8        | 64.3        | 65.7        | 66.5        |
| 0.99                             | 64.9        | 67.1        | 68.3        | 69.2        |
| 0.9                              | 65.0        | 66.9        | 68.1        | 69.2        |
| 0.8                              | <b>65.2</b> | 67.1        | 68.4        | 69.3        |
| 0.7                              | 65.0        | <b>67.1</b> | <b>68.7</b> | <b>69.4</b> |
| 0.6                              | 64.4        | 66.7        | 68.3        | 69.2        |

## B Notations in the Proofs

In the following proofs, we abuse the notation:  $g_i(\mathbf{w}; \mathcal{A}, \mathcal{S}_i) = g(\mathbf{w}; \mathbf{x}_i, \mathcal{A}, \mathcal{S}_i) = \frac{1}{|\mathcal{S}_i|} g(\mathbf{w}; \mathbf{x}_i, \mathcal{A}, \mathcal{S}_i)$  and  $g_i(\mathbf{w}; \mathcal{A}, \mathcal{B}_i) = g(\mathbf{w}; \mathbf{x}_i, \mathcal{A}, \mathcal{B}_i) = \frac{1}{|\mathcal{B}_i|} g(\mathbf{w}; \mathbf{x}_i, \mathcal{A}, \mathcal{B}_i)$ . In the following analysis, we assume  $\mathbf{x}_i \in \mathcal{B}$  is independently sampled with replacement and  $\mathcal{A}, \mathcal{A}'$  are also independently sampled for each sampled data independently though we abuse the same notations  $\mathcal{A}, \mathcal{A}'$  for different data. It is notable that  $\mathbb{E}_{\mathcal{B}_i | \mathbf{x}_i} [g(\mathbf{w}; \mathbf{x}_i, \mathcal{A}, \mathcal{B}_i)] = g(\mathbf{w}; \mathbf{x}_i, \mathcal{A}, \mathcal{S}_i)$ .

We write the objective function as

$$F(\mathbf{w}) = F_1(\mathbf{w}) + F_2(\mathbf{w})$$

where we ignore the constant and

$$F_1(\mathbf{w}) = -\mathbb{E}_{\mathbf{x}_i, \mathcal{A}, \mathcal{A}'} [E(\mathcal{A}(\mathbf{x}_i))^\top E(\mathcal{A}'(\mathbf{x}_i))]$$

$$F_2(\mathbf{w}) = \frac{\tau}{n} \sum_{\mathbf{x}_i \in \mathcal{D}} \mathbb{E}_{\mathcal{A}} \ln (\varepsilon_0 + g(\mathbf{w}; \mathbf{x}_i, \mathcal{A}, \mathcal{S}_i)) = \frac{\tau}{n} \sum_{\mathbf{x}_i \in \mathcal{D}} \mathbb{E}_{\mathcal{A}} f(g(\mathbf{w}; \mathbf{x}_i, \mathcal{A}, \mathcal{S}_i))$$

where  $f(g) = \ln(\varepsilon_0 + g)$ .

## C Proof of Theorem 1

The SimCLR with the update (7) uses the following gradient estimator:

$$\mathbf{v}_t = \nabla F_1(\mathbf{w}_t; \mathcal{B}) + \frac{1}{B} \sum_{\mathbf{x}_i \in \mathcal{B}} \nabla g(\mathbf{w}; \mathbf{x}_i, \mathcal{A}, \mathcal{B}_i) \nabla f(g(\mathbf{w}; \mathbf{x}_i, \mathcal{A}, \mathcal{B}_i))$$

We make the following standard assumptions.

**Assumption 1.** *We assume that there exist  $\sigma, C_g, C_f, L_f, L_F$  such that*

- $\mathbb{E}[\|\nabla F_1(\mathbf{w}; \mathcal{B}) - \nabla F_1(\mathbf{w})\|^2] \leq \frac{\sigma^2}{B}$
- $\mathbb{E}_{\mathcal{B}_i|\mathbf{x}_i}[\|g(\mathbf{w}; \mathbf{x}_i, \mathcal{A}, \mathcal{B}_i) - g(\mathbf{w}; \mathbf{x}_i, \mathcal{A}, \mathcal{S}_i)\|^2] \leq \frac{\sigma^2}{B}$  and  $\mathbb{E}_{\mathcal{B}_i|\mathbf{x}_i}[\|\nabla g(\mathbf{w}; \mathbf{x}_i, \mathcal{A}, \mathcal{B}_i) - \nabla g(\mathbf{w}; \mathbf{x}_i, \mathcal{A}, \mathcal{S}_i)\|^2] \leq \frac{\sigma^2}{B}$
- $\|\nabla g_i(\mathbf{w}; \mathcal{A}, \mathcal{S}_i)\| \leq C_g$
- $\|\nabla f(g)\| \leq C_f$ , and  $\nabla f(\cdot)$  is  $L_f$  Lipschitz continuous
- $F$  is  $L_F$ -smooth.

It is notable that the above assumptions are mild or standard for convergence analysis.

Below, we use  $\mathbb{E}_t$  to denote the expectation over randomness at  $t$ -th iteration given history. First, we have

$$\begin{aligned} \mathbb{E}_t[F(\mathbf{w}_{t+1})] &\leq \mathbb{E}_t[F(\mathbf{w}_t) + (\mathbf{w}_{t+1} - \mathbf{w}_t)^\top \nabla F(\mathbf{w}_t) + \frac{\eta^2 L_F}{2} \|\mathbf{v}_t\|^2] \\ &= F(\mathbf{w}_t) - \eta \mathbb{E}_t[(\nabla F_1(\mathbf{w}_t; \mathcal{B}) + \frac{1}{B} \sum_{\mathbf{x}_i \in \mathcal{B}} \nabla g(\mathbf{w}; \mathbf{x}_i, \mathcal{A}, \mathcal{B}_i) \nabla f(g(\mathbf{w}; \mathbf{x}_i, \mathcal{A}, \mathcal{B}_i)))^\top \nabla F(\mathbf{w}_t) \\ &\quad + \frac{\eta^2 L_F}{2} \|\mathbf{v}_t\|^2] \\ &= F(\mathbf{w}_t) - \eta \mathbb{E}_t[(\nabla F_1(\mathbf{w}_t; \mathcal{B}) + \frac{1}{B} \sum_{\mathbf{x}_i \in \mathcal{B}} \nabla g(\mathbf{w}; \mathbf{x}_i, \mathcal{A}, \mathcal{B}_i) \nabla f(g(\mathbf{w}; \mathbf{x}_i, \mathcal{A}, \mathcal{S}_i)))^\top \nabla F(\mathbf{w}_t)] \\ &\quad + \eta \mathbb{E}_t[(\nabla F_1(\mathbf{w}_t; \mathcal{B}) + \frac{1}{B} \sum_{\mathbf{x}_i \in \mathcal{B}} \nabla g(\mathbf{w}; \mathbf{x}_i, \mathcal{A}, \mathcal{B}_i) \nabla f(g(\mathbf{w}; \mathbf{x}_i, \mathcal{A}, \mathcal{S}_i))) \\ &\quad - (\nabla F_1(\mathbf{w}_t; \mathcal{B}) + \frac{1}{B} \sum_{\mathbf{x}_i \in \mathcal{B}} \nabla g(\mathbf{w}; \mathbf{x}_i, \mathcal{A}, \mathcal{B}_i) \nabla f(g(\mathbf{w}; \mathbf{x}_i, \mathcal{A}, \mathcal{B}_i)))^\top \nabla F(\mathbf{w}_t) \\ &\quad + \frac{\eta^2 L_F}{2} \|\mathbf{v}_t\|^2] \\ &= F(\mathbf{w}_t) - \eta \|\nabla F(\mathbf{w}_t)\|^2 + \eta \mathbb{E}_t[\frac{1}{B} \sum_{\mathbf{x}_i \in \mathcal{B}} \|\nabla F(\mathbf{w}_t)\| C_g L_f \|g(\mathbf{w}; \mathbf{x}_i, \mathcal{A}, \mathcal{B}_i) - g(\mathbf{w}; \mathbf{x}_i, \mathcal{A}, \mathcal{S}_i)\| + \frac{\eta^2 L_F}{2} \|\mathbf{v}_t\|^2] \\ &= F(\mathbf{w}_t) - \eta \|\nabla F(\mathbf{w}_t)\|^2 + \frac{\eta}{2} \|\nabla F(\mathbf{w}_t)\|^2 + \frac{\eta C_g^2 L_f^2}{2} \mathbb{E}_t[\frac{1}{B} \sum_{\mathbf{x}_i \in \mathcal{B}} \|g(\mathbf{w}; \mathbf{x}_i, \mathcal{A}, \mathcal{B}_i) - g(\mathbf{w}; \mathbf{x}_i, \mathcal{A}, \mathcal{S}_i)\|^2] + \frac{\eta^2 L_F}{2} \mathbb{E}_t[\|\mathbf{v}_t\|^2] \\ &= F(\mathbf{w}_t) - \frac{\eta}{2} \|\nabla F(\mathbf{w}_t)\|^2 + \frac{\eta C_g^2 L_f^2 \sigma^2}{2B} + \frac{\eta^2 L_F}{2} \mathbb{E}_t[\|\mathbf{v}_t\|^2] \end{aligned}$$

Then we have

$$\begin{aligned}
& \mathbb{E}[\|\mathbf{v}_t - \nabla F(\mathbf{w}_t)\|^2] = \mathbb{E}[\|\nabla F_1(\mathbf{w}_t; \mathcal{B}) - \nabla F_1(\mathbf{w}_t) \\
& + \frac{1}{B} \sum_{\mathbf{x}_i \in \mathcal{B}} \nabla g(\mathbf{w}; \mathbf{x}_i, \mathcal{A}, \mathcal{B}_i) \nabla f(g(\mathbf{w}; \mathbf{x}_i, \mathcal{A}, \mathcal{B}_i)) - \frac{1}{n} \sum_{\mathbf{x}_i \in \mathcal{D}} \mathbb{E}_{\mathcal{A}} \nabla g(\mathbf{w}; \mathbf{x}_i, \mathcal{A}, \mathcal{S}_i) \nabla f(g(\mathbf{w}; \mathbf{x}_i, \mathcal{A}, \mathcal{S}_i))\|^2] \\
& \leq 2\mathbb{E}[\|\nabla F_1(\mathbf{w}_t; \mathcal{B}) - \nabla F_1(\mathbf{w}_t)\|^2] \\
& + 2\mathbb{E}[\|\frac{1}{B} \sum_{\mathbf{x}_i \in \mathcal{B}} \nabla g(\mathbf{w}; \mathbf{x}_i, \mathcal{A}, \mathcal{B}_i) \nabla f(g(\mathbf{w}; \mathbf{x}_i, \mathcal{A}, \mathcal{B}_i)) - \frac{1}{n} \sum_{\mathbf{x}_i \in \mathcal{D}} \mathbb{E}_{\mathcal{A}} \nabla g(\mathbf{w}; \mathbf{x}_i, \mathcal{A}, \mathcal{S}_i) \nabla f(g(\mathbf{w}; \mathbf{x}_i, \mathcal{A}, \mathcal{S}_i))\|^2] \\
& \leq \frac{2\sigma^2}{B} + 2\mathbb{E}[\|\frac{1}{B} \sum_{\mathbf{x}_i \in \mathcal{B}} \nabla g(\mathbf{w}; \mathbf{x}_i, \mathcal{A}, \mathcal{B}_i) \nabla f(g(\mathbf{w}; \mathbf{x}_i, \mathcal{A}, \mathcal{B}_i)) - \frac{1}{n} \sum_{\mathbf{x}_i \in \mathcal{D}} \mathbb{E}_{\mathcal{A}} \nabla g(\mathbf{w}; \mathbf{x}_i, \mathcal{A}, \mathcal{S}_i) \nabla f(g(\mathbf{w}; \mathbf{x}_i, \mathcal{A}, \mathcal{S}_i))\|^2]
\end{aligned}$$

To bound the second term, we have

$$\begin{aligned}
& \mathbb{E}[\|\frac{1}{B} \sum_{\mathbf{x}_i \in \mathcal{B}} \nabla g(\mathbf{w}; \mathbf{x}_i, \mathcal{A}, \mathcal{B}_i) \nabla f(g(\mathbf{w}; \mathbf{x}_i, \mathcal{A}, \mathcal{B}_i)) - \frac{1}{n} \sum_{\mathbf{x}_i \in \mathcal{D}} \mathbb{E}_{\mathcal{A}} \nabla g(\mathbf{w}; \mathbf{x}_i, \mathcal{A}, \mathcal{S}_i) \nabla f(g(\mathbf{w}; \mathbf{x}_i, \mathcal{A}, \mathcal{S}_i))\|^2] \\
& = \mathbb{E}[\|\frac{1}{B} \sum_{\mathbf{x}_i \in \mathcal{B}} \nabla g(\mathbf{w}; \mathbf{x}_i, \mathcal{A}, \mathcal{B}_i) \nabla f(g(\mathbf{w}; \mathbf{x}_i, \mathcal{A}, \mathcal{B}_i)) - \frac{1}{B} \sum_{\mathbf{x}_i \in \mathcal{B}} \nabla g(\mathbf{w}; \mathbf{x}_i, \mathcal{A}, \mathcal{B}_i) \nabla f(g(\mathbf{w}; \mathbf{x}_i, \mathcal{A}, \mathcal{S}_i)) \\
& + \frac{1}{B} \sum_{\mathbf{x}_i \in \mathcal{B}} \nabla g(\mathbf{w}; \mathbf{x}_i, \mathcal{A}, \mathcal{B}_i) \nabla f(g(\mathbf{w}; \mathbf{x}_i, \mathcal{A}, \mathcal{S}_i)) - \frac{1}{n} \sum_{\mathbf{x}_i \in \mathcal{D}} \mathbb{E}_{\mathcal{A}} \nabla g(\mathbf{w}; \mathbf{x}_i, \mathcal{A}, \mathcal{S}_i) \nabla f(g(\mathbf{w}; \mathbf{x}_i, \mathcal{A}, \mathcal{S}_i))\|^2] \\
& \leq \mathbb{E}[\frac{2}{B^2} B \sum_{\mathbf{x}_i \in \mathcal{B}} C_g^2 L_f^2 \|g(\mathbf{w}; \mathbf{x}_i, \mathcal{A}, \mathcal{B}_i) - g(\mathbf{w}; \mathbf{x}_i, \mathcal{A}, \mathcal{S}_i)\|^2] \\
& + 2\mathbb{E}[\|\frac{1}{B} \sum_{\mathbf{x}_i \in \mathcal{B}} \nabla g(\mathbf{w}; \mathbf{x}_i, \mathcal{A}, \mathcal{B}_i) \nabla f(g(\mathbf{w}; \mathbf{x}_i, \mathcal{A}, \mathcal{S}_i)) - \frac{1}{n} \sum_{\mathbf{x}_i \in \mathcal{D}} \mathbb{E}_{\mathcal{A}} \nabla g(\mathbf{w}; \mathbf{x}_i, \mathcal{A}, \mathcal{S}_i) \nabla f(g(\mathbf{w}; \mathbf{x}_i, \mathcal{A}, \mathcal{S}_i))\|^2] \\
& = \frac{2C_g^2 L_f^2 \sigma^2}{B} \\
& + 2\mathbb{E}[\|\frac{1}{B} \sum_{\mathbf{x}_i \in \mathcal{B}} \nabla g(\mathbf{w}; \mathbf{x}_i, \mathcal{A}, \mathcal{B}_i) \nabla f(g(\mathbf{w}; \mathbf{x}_i, \mathcal{A}, \mathcal{S}_i)) - \frac{1}{B} \sum_{\mathbf{x}_i \in \mathcal{B}} [\nabla g(\mathbf{w}; \mathbf{x}_i, \mathcal{A}, \mathcal{S}_i) \nabla f(g(\mathbf{w}; \mathbf{x}_i, \mathcal{A}, \mathcal{S}_i)) \\
& + \frac{1}{B} \sum_{\mathbf{x}_i \in \mathcal{B}} [\nabla g(\mathbf{w}; \mathbf{x}_i, \mathcal{A}, \mathcal{S}_i) \nabla f(g(\mathbf{w}; \mathbf{x}_i, \mathcal{A}, \mathcal{S}_i)) - \frac{1}{n} \sum_{\mathbf{x}_i \in \mathcal{D}} \mathbb{E}_{\mathcal{A}} \nabla g(\mathbf{w}; \mathbf{x}_i, \mathcal{A}, \mathcal{S}_i) \nabla f(g(\mathbf{w}; \mathbf{x}_i, \mathcal{A}, \mathcal{S}_i))\|^2] \\
& = \frac{2C_g^2 L_f^2 \sigma^2}{B} + \frac{4C_f^2 \sigma^2}{B} \\
& + 4\mathbb{E}[\|\frac{1}{B} \sum_{\mathbf{x}_i \in \mathcal{B}} [\nabla g(\mathbf{w}; \mathbf{x}_i, \mathcal{A}, \mathcal{S}_i) \nabla f(g(\mathbf{w}; \mathbf{x}_i, \mathcal{A}, \mathcal{S}_i)) - \frac{1}{n} \sum_{\mathbf{x}_i \in \mathcal{D}} \mathbb{E}_{\mathcal{A}} \nabla g(\mathbf{w}; \mathbf{x}_i, \mathcal{A}, \mathcal{S}_i) \nabla f(g(\mathbf{w}; \mathbf{x}_i, \mathcal{A}, \mathcal{S}_i))\|^2] \\
& \leq \frac{2C_g^2 L_f^2 \sigma^2}{B} + \frac{4C_f^2 \sigma^2}{B} \\
& + 4\mathbb{E}[\|\frac{1}{B} \sum_{\mathbf{x}_i \in \mathcal{B}} [\nabla g(\mathbf{w}; \mathbf{x}_i, \mathcal{A}, \mathcal{S}_i) \nabla f(g(\mathbf{w}; \mathbf{x}_i, \mathcal{A}, \mathcal{S}_i))\|^2] \\
& \leq \frac{2C_g^2 L_f^2 \sigma^2}{B} + \frac{4C_f^2 \sigma^2}{B} + 4C_g^2 C_f^2
\end{aligned}$$

As a result,

$$\mathbb{E}[\|\mathbf{v}_t\|^2] \leq 2\|\nabla F(\mathbf{w}_t)\|^2 + \frac{C}{B} + 16C_g^2 C_f^2,$$

where  $C$  is a proper constant. By combining the above results together, we have

$$\mathbb{E}[F(\mathbf{w}_{t+1})] \leq F(\mathbf{w}_t) - \frac{\eta}{2} \|\nabla F(\mathbf{w}_t)\|^2 + \frac{\eta C}{B} + \eta^2 L_F \|\nabla F(\mathbf{w}_t)\|^2 + 16\eta^2 L_F C_g^2 C_f^2.$$

Then with  $\eta L_F \leq 1/4$ , we have

$$\mathbb{E}\left[\frac{1}{T} \sum_{t=1}^T \|\nabla F(\mathbf{w}_t)\|^2\right] \leq \frac{4(F(\mathbf{w}_1) - F_*)}{\eta T} + 64\eta L_f C_f^2 C_g^2 + \frac{4C}{B},$$

which finises the proof.

We can also sharpen the bound of  $\mathbb{E}[\|\mathbf{v}_t - \nabla F(\mathbf{w}_t)\|^2]$  by noting that

$$\begin{aligned} & \mathbb{E}\left[\left\|\frac{1}{B} \sum_{\mathbf{x}_i \in \mathcal{B}} [\nabla g(\mathbf{w}; \mathbf{x}_i, \mathcal{A}, \mathcal{S}_i) \nabla f(g(\mathbf{w}; \mathbf{x}_i, \mathcal{A}, \mathcal{S}_i)) - \frac{1}{n} \sum_{\mathbf{x}_i \in \mathcal{D}} \mathbb{E}_{\mathcal{A}} \nabla g(\mathbf{w}; \mathbf{x}_i, \mathcal{A}, \mathcal{S}_i) \nabla f(g(\mathbf{w}; \mathbf{x}_i, \mathcal{A}, \mathcal{S}_i))]\right\|^2\right] \\ &= \mathbb{E}\left[\left\|\frac{1}{B} \sum_{\mathbf{x}_i \in \mathcal{B}} [\nabla g(\mathbf{w}; \mathbf{x}_i, \mathcal{A}, \mathcal{S}_i) \nabla f(g(\mathbf{w}; \mathbf{x}_i, \mathcal{A}, \mathcal{S}_i)) - \frac{1}{B} \sum_{\mathbf{x}_i \in \mathcal{B}} \mathbb{E}_{\mathcal{A}} [\nabla g(\mathbf{w}; \mathbf{x}_i, \mathcal{A}, \mathcal{S}_i) \nabla f(g(\mathbf{w}; \mathbf{x}_i, \mathcal{A}, \mathcal{S}_i))]\right. \right. \\ & \quad \left. \left. - \frac{1}{B} \sum_{\mathbf{x}_i \in \mathcal{B}} \mathbb{E}_{\mathcal{A}} [\nabla g(\mathbf{w}; \mathbf{x}_i, \mathcal{A}, \mathcal{S}_i) \nabla f(g(\mathbf{w}; \mathbf{x}_i, \mathcal{A}, \mathcal{S}_i))] - \frac{1}{n} \sum_{\mathbf{x}_i \in \mathcal{D}} \mathbb{E}_{\mathcal{A}} \nabla g(\mathbf{w}; \mathbf{x}_i, \mathcal{A}, \mathcal{S}_i) \nabla f(g(\mathbf{w}; \mathbf{x}_i, \mathcal{A}, \mathcal{S}_i))]\right\|^2\right] \\ & \leq \frac{4C_g^2 C_f^2}{B}. \end{aligned}$$

As a result,  $\mathbb{E}[\|\mathbf{v}_t - \nabla F(\mathbf{w}_t)\|^2] \leq \frac{2C_g^2 L_f^2 \sigma^2}{B} + \frac{4C_f^2 \sigma^2}{B} + \frac{4C_g^2 C_f^2}{B}$ , then with  $\eta L_F \leq 1/4$ , we have

$$\mathbb{E}\left[\frac{1}{T} \sum_{t=1}^T \|\nabla F(\mathbf{w}_t)\|^2\right] \leq \frac{4(F(\mathbf{w}_1) - F_*)}{\eta T} + \frac{C}{B},$$

which still has a dependence of  $1/B$ . However, we can set  $\eta = O(1)$  and  $T = O(1/\epsilon^2)$ ,  $B = O(1/\epsilon^2)$  in order to achieve an  $\epsilon$ -stationary solution.

## D Proof of Theorem 2

First, we note that the gradient estimator  $\mathbf{m}_t$  is

$$\begin{aligned} \mathbf{m}_t &= \nabla F_1(\mathbf{w}_t; \mathcal{B}) + \frac{1}{B} \sum_{\mathbf{x}_i \in \mathcal{B}} \nabla f(u_{i,t}) \underbrace{\frac{1}{2}(\nabla g(\mathbf{w}_t; \mathbf{x}_i, \mathcal{A}, \mathcal{B}_i) + \nabla g(\mathbf{w}_t; \mathbf{x}_i, \mathcal{A}', \mathcal{B}_i))}_{\nabla g_i(\mathbf{w}_t; \mathcal{A}, \mathcal{A}', \mathcal{B}_i)} \\ \mathbf{u}_{i,t+1} &= (1 - \gamma) \mathbf{u}_{i,t} + \underbrace{\gamma \frac{1}{2}(g(\mathbf{w}_t; \mathbf{x}_i, \mathcal{A}, \mathcal{B}_i) + g(\mathbf{w}_t; \mathbf{x}_i, \mathcal{A}', \mathcal{B}_i))}_{g_i(\mathbf{w}_t; \mathcal{A}, \mathcal{A}', \mathcal{B}_i)} \end{aligned}$$

Define  $g_i(\mathbf{w}) = \mathbb{E}_{\mathcal{A}}[g(\mathbf{w}; \mathbf{x}_i, \mathcal{A}, \mathcal{S}_i)]$ . We can see that  $\mathbb{E}_{\mathcal{B}_i, \mathcal{A}, \mathcal{A}' | \mathbf{x}_i}[g_i(\mathbf{w}_t; \mathcal{A}, \mathcal{A}', \mathcal{B}_i)] = g_i(\mathbf{w}_t)$ , and  $\mathbb{E}_{\mathcal{B}_i, \mathcal{A}, \mathcal{A}' | \mathbf{x}_i}[\nabla g_i(\mathbf{w}_t; \mathcal{A}, \mathcal{A}', \mathcal{B}_i)] = \nabla g_i(\mathbf{w}_t)$ .

We make the following assumptions.

**Assumption 2.** We assume that there exist  $\sigma, C_g, C_f, L_F$  such that

- $\mathbb{E}[\|\nabla F_1(\mathbf{w}; \mathcal{B}) - \nabla F_1(\mathbf{w})\|^2] \leq \frac{\sigma^2}{B}$
- $\mathbb{E}_{\mathcal{B}_i | \mathbf{x}_i}[\|g(\mathbf{w}; \mathbf{x}_i, \mathcal{A}, \mathcal{B}_i) - g(\mathbf{w}; \mathbf{x}_i, \mathcal{A}, \mathcal{S}_i)\|^2] \leq \frac{\sigma^2}{B}$  and  $\mathbb{E}_{\mathcal{B}_i | \mathbf{x}_i}[\|\nabla g(\mathbf{w}; \mathbf{x}_i, \mathcal{A}, \mathcal{B}_i) - \nabla g(\mathbf{w}; \mathbf{x}_i, \mathcal{A}, \mathcal{S}_i)\|^2] \leq \frac{\sigma^2}{B}$
- $\|\nabla f(g)\| \leq C_f$ ,  $\|\nabla g_i(\mathbf{w})\| \leq C_g$ ,  $\|\nabla F_1(\mathbf{w})\| \leq C_{F_1}$ ,  $\|\nabla g_i(\mathbf{w}; \mathcal{A}, \mathcal{S}_i)\| \leq C_g$
- $\nabla f(\cdot)$  is  $L_f$  Lipschitz continuous
- $F$  is  $L_F$ -smooth.
- $\|E(\mathbf{z})\| \leq 1$ ,  $\forall \mathbf{z}$

- $\mathbb{E}_{\mathcal{A}, \mathcal{A}'} \mathbb{E}_{\mathbf{z} \sim \mathcal{S}_i} |E(\mathcal{A}(\mathbf{x}_i))^\top E(\mathbf{z})] - E(\mathcal{A}'(\mathbf{x}_i))^\top E(\mathbf{z})|^2 \leq \epsilon^2$  for any  $\mathbf{x}_i \in \mathcal{D}$

We note that under the above assumption we have

$$\begin{aligned}
& \mathbb{E}_{\mathcal{A}, \mathcal{A}'} \|g_i(\mathbf{w}_t; \mathcal{A}', \mathcal{S}_i) - g_i(\mathbf{w}_t; \mathcal{A}, \mathcal{S}_i)\|^2 \\
&= \mathbb{E}_{\mathcal{A}, \mathcal{A}'} \|\mathbb{E}_{\mathbf{z} \sim \mathcal{S}_i} (\exp(E(\mathcal{A}(\mathbf{x}_i))^\top E(\mathbf{z})/\tau) - \mathbb{E}_{\mathbf{z} \sim \mathcal{S}_i} (\exp(E(\mathcal{A}'(\mathbf{x}_i))^\top E(\mathbf{z})/\tau))\|^2 \\
&\leq \mathbb{E}_{\mathcal{A}, \mathcal{A}'} \mathbb{E}_{\mathbf{z} \sim \mathcal{S}_i} \|(\exp(E(\mathcal{A}(\mathbf{x}_i))^\top E(\mathbf{z})/\tau) - (\exp(E(\mathcal{A}'(\mathbf{x}_i))^\top E(\mathbf{z})/\tau))\|^2 \\
&\leq C \mathbb{E}_{\mathcal{A}, \mathcal{A}'} \mathbb{E}_{\mathbf{z} \sim \mathcal{S}_i} \|E(\mathcal{A}(\mathbf{x}_i))^\top E(\mathbf{z})/\tau - E(\mathcal{A}'(\mathbf{x}_i))^\top E(\mathbf{z})/\tau\|^2 \\
&\leq O(\epsilon^2)
\end{aligned}$$

where  $C$  is a proper constant that bounds the Lipschitz of  $\exp(E(\cdot)/\tau)$ .

We need the following lemma, whose proof can be found in [13] and thus is omitted here.

**Lemma 1.** Consider a sequence  $\mathbf{w}_{t+1} = \mathbf{w}_t - \eta \mathbf{v}_t$  and the  $L_F$ -smooth function  $F$  and the step size  $\eta_t L_F \leq 1/2$ .

$$F(\mathbf{w}_{t+1}) \leq F(\mathbf{w}_t) + \frac{\eta}{2} \|\Delta_t\|^2 - \frac{\eta}{2} \|\nabla F(\mathbf{w}_t)\|^2 - \frac{\eta}{4} \|\mathbf{v}_t\|^2, \quad (15)$$

where  $\Delta_t = \mathbf{v}_t - \nabla F(\mathbf{w}_t)$ .

**Lemma 2.** Assume  $\mathbb{E}_{\mathcal{A}, \mathcal{A}'} \|g_i(\mathbf{w}_t; \mathcal{A}', \mathcal{S}_i) - g_i(\mathbf{w}_t; \mathcal{A}, \mathcal{S}_i)\|^2 \leq \epsilon^2$ , we have

$$\begin{aligned}
\mathbb{E}[\|\Delta_t\|^2] &\leq (1 - \beta) \mathbb{E}[\|\Delta_{t-1}\|^2] + \frac{2L_F^2 \eta^2 \mathbb{E}[\|\mathbf{v}_{t-1}\|^2]}{\beta} + \frac{14\beta L_f^2 C_g^2}{n} \mathbb{E}[\|\Xi_t\|^2] + \frac{14\beta L_f^2 C_g^2}{n} \mathbb{E}[\|\mathbf{u}_t - \mathbf{u}_{t+1}\|^2] \\
&\quad + \frac{\beta^2 C}{B} + 5\beta C_g^2 L_f^2 \epsilon^2.
\end{aligned}$$

where  $\Delta_t = \mathbf{v}_t - \nabla F(\mathbf{w}_t)$ ,  $\Xi_t = \mathbf{u}_{t+1} - \mathbf{g}(\mathbf{w}_t)$ ,  $\mathbf{g}(\mathbf{w}) = (g_1(\mathbf{w}), \dots, g_n(\mathbf{w}))$ , and  $C$  is a proper constant.

*Proof.* We define that  $\Delta_t = \mathbf{v}_t - \nabla F(\mathbf{w}_t)$ . Below, for the analysis of  $\Delta_t$ , we note that  $\mathbf{u}_t$  is independent of the randomness in  $\mathcal{B}, \mathcal{A}, \mathcal{A}'$ . Based on the update rule  $\mathbf{v}_t = (1 - \beta)\mathbf{v}_{t-1} + \beta\mathbf{m}_t$ , we have

$$\begin{aligned}
\|\Delta_t\|^2 &= \|\mathbf{v}_t - \nabla F(\mathbf{w}_t)\|^2 \\
&= \left\| (1 - \beta)\mathbf{v}_{t-1} + \beta(\nabla F_1(\mathbf{w}_t; \mathcal{B}) + \frac{1}{B} \sum_{i \in \mathcal{B}} \nabla f([\mathbf{u}_{t-1}]_i) \nabla g_i(\mathbf{w}_t; \mathcal{A}, \mathcal{A}', \mathcal{B}_i)) - \nabla F(\mathbf{w}_t) \right\|^2 \\
&= \underbrace{\|(1 - \beta)(\mathbf{v}_{t-1} - \nabla F(\mathbf{w}_{t-1}))\|}_{A_1} + \underbrace{\|(1 - \beta)(\nabla F(\mathbf{w}_{t-1}) - \nabla F(\mathbf{w}_t))\|}_{A_2} \\
&\quad + \underbrace{\beta \left( \frac{1}{B} \sum_{i \in \mathcal{B}} \nabla f(g_i(\mathbf{w}_t)) \nabla g_i(\mathbf{w}_t; \mathcal{A}, \mathcal{A}', \mathcal{B}_i) - \frac{1}{B} \sum_{i \in \mathcal{B}} \frac{1}{2} \sum_{\mathbf{a} \in \mathcal{A}, \mathcal{A}'} \nabla f(g_i(\mathbf{w}_t; \mathbf{a}, \mathcal{S}_i)) \nabla g_i(\mathbf{w}_t; \mathbf{a}, \mathcal{B}_i) \right)}_{A_3} \\
&\quad + \underbrace{\beta \left( \frac{1}{B} \sum_{i \in \mathcal{B}} \nabla f([\mathbf{u}_{t-1}]_i) \nabla g_i(\mathbf{w}_t; \mathcal{A}, \mathcal{A}', \mathcal{B}_i) - \frac{1}{B} \sum_{i \in \mathcal{B}} \nabla f(g_i(\mathbf{w}_t)) \nabla g_i(\mathbf{w}_t; \mathcal{A}, \mathcal{A}', \mathcal{B}_i) \right)}_{A_4} \\
&\quad + \underbrace{\beta \left( \nabla F_1(\mathbf{w}_t; \mathcal{B}) + \frac{1}{2B} \sum_{i \in \mathcal{B}} (\nabla f(g_i(\mathbf{w}_t; \mathcal{A}, \mathcal{S}_i)) \nabla g_i(\mathbf{w}_t; \mathcal{A}, \mathcal{B}_i) + \nabla f(g_i(\mathbf{w}_t; \mathcal{A}', \mathcal{S}_i)) \nabla g_i(\mathbf{w}_t; \mathcal{A}', \mathcal{B}_i)) - \nabla F(\mathbf{w}_t) \right)}_{A_5} \\
\end{aligned}$$

Note that  $\mathbb{E} [\langle A_1, A_5 \rangle] = \mathbb{E} [\langle A_2, A_5 \rangle] = 0$ . Then,

$$\begin{aligned} \mathbb{E}_t [\|A_1 + A_2 + A_3 + A_4 + A_5\|^2] &= \|A_1\|^2 + \|A_2\|^2 + \mathbb{E}_t [\|A_3\|^2] + \mathbb{E}_t [\|A_4\|^2] + \mathbb{E}_t [\|A_5\|^2] + 2\langle A_1, A_2 \rangle \\ &+ 2\mathbb{E}_t [\langle A_1, A_3 \rangle] + 2\mathbb{E}_t [\langle A_1, A_4 \rangle] + 2\mathbb{E}_t [\langle A_2, A_3 \rangle] + 2\mathbb{E}_t [\langle A_2, A_4 \rangle] + 2\mathbb{E}_t [\langle A_3, A_4 \rangle] + 2\mathbb{E}_t [\langle A_3, A_5 \rangle] + 2\mathbb{E}_t [\langle A_4, A_5 \rangle]. \end{aligned}$$

Based on Young's inequality for products, we have  $2\langle \mathbf{a}, \mathbf{b} \rangle \leq \frac{\|\mathbf{a}\|^2 c}{2} + \frac{2\|\mathbf{b}\|^2}{c}$  for  $c > 0$ .

$$\begin{aligned} \mathbb{E}_t [\|A_1 + A_2 + A_3 + A_4 + A_5\|^2] \\ \leq (1 + \beta) \|A_1\|^2 + (3 + 3/\beta) \|A_2\|^2 + (4 + 3/\beta) \mathbb{E}_t [\|A_3\|^2] + (4 + \frac{3}{\beta}) \mathbb{E}_t [\|A_4\|^2] + 3\mathbb{E}_t [\|A_5\|^2]. \end{aligned}$$

Thus, we have

$$\mathbb{E}_t [\|\Delta_t\|^2] \leq (1 - \beta) \|\Delta_{t-1}\|^2 + (3 + 3/\beta) \|A_2\|^2 + (4 + 3/\beta) \mathbb{E}_t [\|A_3\|^2] + (4 + 3/\beta) \mathbb{E}_t [\|A_4\|^2] + 3\mathbb{E}_t [\|A_5\|^2]. \quad (16)$$

Moreover, we have

$$\|A_2\|^2 = (1 - \beta)^2 \|\nabla F(\mathbf{w}_{t-1}) - \nabla F(\mathbf{w}_t)\|^2 \leq (1 - \beta)^2 \eta^2 L_F^2 \|\mathbf{v}_{t-1}\|^2, \quad (17)$$

$$\begin{aligned} \mathbb{E}_t [\|A_3\|^2] &\leq \beta^2 C_g^2 L_f^2 \mathbb{E}_{\mathcal{A}} \|g_i(\mathbf{w}_t) - g_i(\mathbf{w}_t; \mathcal{A}, \mathcal{S}_i)\|^2 \leq \beta^2 C_g^2 L_f^2 \mathbb{E}_{\mathcal{A}} \|\mathbb{E}_{\mathcal{A}'} g_i(\mathbf{w}_t; \mathcal{A}', \mathcal{S}_i) - g_i(\mathbf{w}_t; \mathcal{A}, \mathcal{S}_i)\|^2 \\ &\leq \beta^2 C_g^2 L_f^2 \mathbb{E}_{\mathcal{A}, \mathcal{A}'} \|g_i(\mathbf{w}_t; \mathcal{A}', \mathcal{S}_i) - g_i(\mathbf{w}_t; \mathcal{A}, \mathcal{S}_i)\|^2 \end{aligned} \quad (18)$$

$$\mathbb{E}_t [\|A_4\|^2] \leq \mathbb{E}_t [\frac{\beta^2}{B} \sum_{i \in \mathcal{B}} \|\nabla g_i(\mathbf{w}_t; \mathcal{A}, \mathcal{A}', \mathcal{B}_i)\|^2 \|\nabla f([\mathbf{u}_{t-1}]_i) - \nabla f(g_i(\mathbf{w}_t))\|^2] \quad (19)$$

$$\begin{aligned} &\leq \mathbb{E}_t [\frac{\beta^2 L_f^2}{B} \sum_{i \in \mathcal{B}} \|\nabla g_i(\mathbf{w}_t; \mathcal{A}, \mathcal{A}', \mathcal{B}_i)\|^2 \|[\mathbf{u}_{t-1}]_i - g_i(\mathbf{w}_t)\|^2] \\ &\leq \beta^2 L_f^2 C_g^2 \mathbb{E}_t \left[ \frac{1}{B} \sum_{i \in \mathcal{B}} \|[\mathbf{u}_{t-1}]_i - g_i(\mathbf{w}_t)\|^2 \right] \end{aligned} \quad (20)$$

Since the update rule of  $\mathbf{u}_t$  is based on  $\mathcal{B}$ , we have

$$\mathbb{E}_t \left[ \frac{1}{B} \sum_{i \in \mathcal{B}} \|[\mathbf{u}_{t-1}]_i - g_i(\mathbf{w}_t)\|^2 \right] = \frac{1}{n} \mathbb{E}_t [\|\mathbf{u}_{t-1} - \mathbf{g}(\mathbf{w}_t)\|^2],$$

where and  $\mathbf{g}(\mathbf{w}_t) := [g_1(\mathbf{w}_t), \dots, g_n(\mathbf{w}_t)]^\top$ . Then,  $\|\mathbf{u}_{t-1} - \mathbf{g}(\mathbf{w}_t)\|^2 = \sum_{i \in \mathcal{D}} \|[\mathbf{u}_{t-1}]_i - g_i(\mathbf{w}_t)\|^2$ . Thus, we also have

$$\begin{aligned} \mathbb{E}_t [\|A_5\|^2] &\leq \frac{2\beta^2 \sigma^2}{B} \\ &+ 2\beta^2 \mathbb{E}_t \left[ \left\| \left( \frac{1}{2B} \sum_{i \in \mathcal{B}} (\nabla f(g_i(\mathbf{w}_t; \mathcal{A}, \mathcal{S}_i)) \nabla g_i(\mathbf{w}_t; \mathcal{A}, \mathcal{B}_i) + \nabla f(g_i(\mathbf{w}_t; \mathcal{A}', \mathcal{S}_i)) \nabla g_i(\mathbf{w}_t; \mathcal{A}', \mathcal{B}_i)) - \nabla F_2(\mathbf{w}_t) \right) \right\|^2 \right] \\ &\leq \frac{2\beta^2 \sigma^2}{B} + 4\beta^2 \mathbb{E}_t \left[ \frac{1}{B} \sum_{i \in \mathcal{B}} \mathbb{E}_{\mathcal{B}_i} \|(\nabla f(g_i(\mathbf{w}_t; \mathcal{A}, \mathcal{S}_i)) \nabla g_i(\mathbf{w}_{t+1}; \mathcal{A}, \mathcal{B}_i) - \mathbb{E}_{\mathcal{B}_i} \nabla f(g_i(\mathbf{w}_t; \mathcal{A}, \mathcal{S}_i)) \nabla g_i(\mathbf{w}_t; \mathcal{A}, \mathcal{B}_i))\|^2 \right] \\ &+ 8\beta^2 \mathbb{E}_{\mathcal{B}} \left[ \frac{1}{B} \sum_{i \in \mathcal{B}} \mathbb{E}_{\mathcal{A}} \|\nabla f(g_i(\mathbf{w}_t; \mathcal{A}, \mathcal{S}_i)) \nabla g_i(\mathbf{w}_t; \mathcal{A}, \mathcal{S}_i) - \mathbb{E}_{\mathcal{A}} \nabla f(g_i(\mathbf{w}_t; \mathcal{A}, \mathcal{S}_i)) \nabla g_i(\mathbf{w}_t; \mathcal{A}, \mathcal{S}_i)\|^2 \right] \\ &+ 8\beta^2 \mathbb{E}_{\mathcal{B}} \left[ \left\| \frac{1}{B} \sum_{i \in \mathcal{B}} \mathbb{E}_{\mathcal{A}} \nabla f(g_i(\mathbf{w}_t; \mathcal{A}, \mathcal{S}_i)) \nabla g_i(\mathbf{w}_t; \mathcal{A}, \mathcal{S}_i) - \frac{1}{n} \sum_{i \in \mathcal{D}} \mathbb{E}_{\mathcal{A}} \nabla f(g_i(\mathbf{w}_t; \mathcal{A}, \mathcal{S}_i)) \nabla g_i(\mathbf{w}_t; \mathcal{A}, \mathcal{S}_i) \right\|^2 \right] \\ &\leq \frac{\beta^2 C}{B}, \end{aligned} \quad (21)$$

where  $C$  is some proper constant.

Define that  $\Xi_t = \mathbb{E} \left[ \frac{1}{n} \|\mathbf{u}_t - \mathbf{g}(\mathbf{w}_t)\|^2 \right]$ . By combining the above inequalities we have

$$\begin{aligned} \mathbb{E}[\|\Delta_t\|^2] &\leq (1 - \beta) \mathbb{E}[\|\Delta_{t-1}\|^2] + \frac{3L_f^2 \eta^2 \mathbb{E}[\|\mathbf{v}_{t-1}\|^2]}{\beta} + \frac{14\beta L_f^2 C_g^2}{n} \mathbb{E}[\|\Xi_t\|^2] + 14\beta L_f^2 C_g^2 \mathbb{E}[\|\mathbf{u}_t - \mathbf{u}_{t-1}\|^2] \\ &\quad + \frac{\beta^2 C}{B} + 7\beta C_g^2 L_f^2 \epsilon^2. \end{aligned}$$

□

**Lemma 3.** *If  $\gamma \leq 1/5$ , the following equation holds.*

$$\mathbb{E}[\Xi_{t+1}] \leq \left(1 - \frac{\gamma B}{4n}\right) \mathbb{E}[\Xi_t] + \frac{5n\eta^2 C_g^2 \mathbb{E}[\|\mathbf{v}_t\|^2]}{\gamma B} + \frac{2\gamma^2 \sigma^2 B}{nB} - \frac{1}{4n} \mathbb{E}[\|\mathbf{u}_{t+1} - \mathbf{u}_t\|^2]. \quad (22)$$

By Combining Lemma 1, 2, and Lemma 3, we can prove the final theorem.

$$\mathbb{E}[F(\mathbf{w}_{t+1}) - F^*] \leq \mathbb{E}[F(\mathbf{w}_t) - F^*] + \frac{\eta}{2} \mathbb{E}[\Delta_t] - \frac{\eta}{2} \mathbb{E}[\|\nabla F(\mathbf{w}_t)\|^2] - \frac{\eta}{4} \mathbb{E}[\|\mathbf{v}_t\|^2] \quad (23)$$

$$\begin{aligned} \mathbb{E}[\Delta_{t+1}] &\leq (1 - \beta) \mathbb{E}[\Delta_t] + \frac{3L_f^2 \eta^2}{\beta} \mathbb{E}[\|\mathbf{v}_t\|^2] + 14\beta L_f^2 C_g^2 \mathbb{E}[\Xi_{t+1}] + \frac{\beta^2 C}{B} + \frac{14\beta L_f^2 C_g^2}{n} \mathbb{E}[\|\mathbf{u}_{t+1} - \mathbf{u}_t\|^2] \\ &\quad + 7\beta C_g^2 L_f^2 \epsilon^2 \end{aligned} \quad (24)$$

$$\mathbb{E}[\Xi_{t+1}] \leq \left(1 - \frac{\gamma B}{4n}\right) \mathbb{E}[\Xi_t] + \frac{5n\eta^2 C_g^2 \mathbb{E}[\|\mathbf{v}_t\|^2]}{\gamma B} + \frac{2\gamma^2 \sigma^2 B}{nB} - \frac{1}{4n} \mathbb{E}[\|\mathbf{u}_{t+1} - \mathbf{u}_t\|^2]. \quad (25)$$

Summing (23),  $\frac{\eta}{\beta} \times (24)$ , and  $\frac{56L_f^2 C_g^2 n \eta}{\gamma B} \times (25)$  leads to

$$\begin{aligned} &\mathbb{E} \left[ (F(\mathbf{w}_{t+1}) - F^*) + \frac{\eta}{\beta} \Delta_{t+1} + \frac{56L_f^2 C_g^2 n \eta}{\gamma B} \left(1 - \frac{\gamma B}{4n}\right) \Xi_{t+1} \right] \\ &\leq \mathbb{E} \left[ (F(\mathbf{w}_t) - F^*) + \frac{\eta}{\beta} \left(1 - \frac{\beta}{2}\right) \Delta_t + \frac{56L_f^2 C_g^2 n \eta}{\gamma B} \left(1 - \frac{\gamma B}{4n}\right) \Xi_t \right] - L_f^2 C_g^2 \eta \left(\frac{14n}{\gamma B} - 14\right) \mathbb{E} \left[ \frac{1}{n} \|\mathbf{u}_{t+1} - \mathbf{u}_t\|^2 \right] \\ &\quad - \frac{\eta}{2} \mathbb{E}[\|\nabla F(\mathbf{w}_t)\|^2] - \eta \left(\frac{1}{4} - \frac{3L_f^2 \eta^2}{\beta^2} - \frac{280L_f^2 n^2 C_g^4 \eta^2}{\gamma^2 B^2}\right) \mathbb{E}[\|\mathbf{v}_t\|^2] + \frac{\beta \eta C}{B} + \frac{112\eta \gamma L_f^2 C_g^2 \sigma^2}{B} + 7\eta C_g^2 L_f^2 \epsilon^2. \end{aligned}$$

If  $\gamma \leq \frac{n}{B}$ , we have  $\frac{14n}{\gamma B} - 14 \geq 0$ . Set  $\beta = O(\min(B\epsilon^2, \frac{2}{7}))$ ,  $\gamma = \min\{O(B\epsilon^2), \frac{5n}{14B}\}$ , and  $\eta = \min\left\{\frac{\beta}{6L_f}, \frac{\gamma B}{50L_f n C_g^2}\right\}$ . Define the Lyapunov function as  $\Phi_t := (F(\mathbf{w}_t) - F^*) + \frac{\eta}{\beta} \Delta_t + \frac{56L_f^2 C_g^2 \eta}{B} \left(1 - \frac{\gamma B}{4n}\right) \Xi_t$ . If we initialize  $\mathbf{v}_0 = 0$ , we have  $\mathbb{E}[\Delta_1] \leq 2C_{F_1} + 2C_f^2 C_g^2$ . Then,

$$\frac{1}{T} \sum_{t=1}^T \mathbb{E}[\|\nabla F(\mathbf{w}_t)\|^2] \leq \frac{2\Lambda_\Phi^1}{\eta T} + \frac{2\beta C}{B} + \frac{224\gamma L_f^2 C_g^2 \sigma^2}{B} + 14C_g^2 L_f^2 \epsilon^2, \quad (26)$$

where we define  $\mathbb{E}[\Phi_1] \leq \Delta_F + \frac{1}{6L_f} (2C_{F_1}^2 + 2C_f^2 C_g^2) + \frac{C\Xi_1}{n} =: \Lambda_\Phi^1$ . After  $T = O(\max(\frac{n}{B^2 \epsilon^4}, \frac{1}{B \epsilon^4}))$  iterations, we have  $\frac{1}{T} \sum_{t=1}^T \mathbb{E}[\|\nabla F(\mathbf{w}_t)\|^2] \leq O(\epsilon^2)$ .

## E Proof of Corollary 1

The proof is similar to that of Theorem 2, except that the bound  $\Delta_t$ , which is shown below.

$$\begin{aligned}
\|\Delta_t\|^2 &= \|\mathbf{v}_t - \nabla F(\mathbf{w}_t)\|^2 \\
&= \left\| (1-\beta)\mathbf{v}_{t-1} + \beta(\nabla F_1(\mathbf{w}_t; \mathcal{B}) + \frac{1}{B} \sum_{i \in \mathcal{B}} \nabla f(g_i(\mathbf{w}_t; \mathcal{A}, \mathcal{B}_i)) \nabla g_i(\mathbf{w}_t; \mathcal{A}, \mathcal{B}_i)) - \nabla F(\mathbf{w}_t) \right\|^2 \\
&= \left\| \underbrace{(1-\beta)(\mathbf{v}_{t-1} - \nabla F(\mathbf{w}_{t-1}))}_{A_1} + \underbrace{(1-\beta)(\nabla F(\mathbf{w}_{t-1}) - \nabla F(\mathbf{w}_t))}_{A_2} \right. \\
&\quad \left. + \beta \underbrace{\left( \frac{1}{B} \sum_{i \in \mathcal{B}} \nabla f(g_i(\mathbf{w}_t; \mathcal{A}, \mathcal{B}_i)) \nabla g_i(\mathbf{w}_{t+1}; \mathcal{A}, \mathcal{B}_i) - \frac{1}{B} \sum_{i \in \mathcal{B}} \nabla f(g_i(\mathbf{w}_t; \mathcal{A}, \mathcal{S}_i)) \nabla g_i(\mathbf{w}_t; \mathcal{A}, \mathcal{B}_i) \right)}_{A_3} \right. \\
&\quad \left. + \beta \underbrace{\left( \nabla F_1(\mathbf{w}_t; \mathcal{B}) + \frac{1}{B} \sum_{i \in \mathcal{B}} \nabla f(g_i(\mathbf{w}_t; \mathcal{A}, \mathcal{S}_i)) \nabla g_i(\mathbf{w}_t; \mathcal{A}, \mathcal{B}_i) - \nabla F(\mathbf{w}_t) \right)}_{A_4} \right\|^2.
\end{aligned}$$

Note that  $\mathbb{E}[\langle A_1, A_4 \rangle] = \mathbb{E}[\langle A_2, A_4 \rangle] = 0$ . Then,

$$\begin{aligned}
\mathbb{E}_t [\|A_1 + A_2 + A_3 + A_4\|^2] &= \|A_1\|^2 + \|A_2\|^2 + \mathbb{E}_t [\|A_3\|^2] + \mathbb{E}_t [\|A_4\|^2] + 2\langle A_1, A_2 \rangle \\
&\quad + 2\mathbb{E}_t [\langle A_1, A_3 \rangle] + 2\mathbb{E}_t [\langle A_1, A_4 \rangle] + 2\mathbb{E}_t [\langle A_2, A_3 \rangle] + 2\mathbb{E}_t [\langle A_2, A_4 \rangle] + 2\mathbb{E}_t [\langle A_3, A_4 \rangle]
\end{aligned}$$

Based on Young's inequality for products, we have  $2\langle \mathbf{a}, \mathbf{b} \rangle \leq \frac{\|\mathbf{a}\|^2 c}{2} + \frac{2\|\mathbf{b}\|^2}{c}$  for  $c > 0$ .

$$\begin{aligned}
\mathbb{E}_t [\|A_1 + A_2 + A_3 + A_4 + A_5\|^2] &\leq (1+\beta)\|A_1\|^2 + C/\beta\|A_2\|^2 + C/\beta\mathbb{E}_t [\|A_3\|^2] + C\mathbb{E}_t [\|A_4\|^2],
\end{aligned}$$

where  $C$  is a proper constant. We can show that  $\mathbb{E}[\|A_3\|^2] \leq \beta^2 \frac{C}{B}$  and  $\mathbb{E}[\|A_4\|^2] \leq \beta^2 \frac{C}{B}$  for some constant  $C$ . Then we have

$$\mathbb{E}[\|\Delta_t\|^2] \leq (1-\beta)\mathbb{E}[\|\Delta_{t-1}\|^2] + \frac{C\eta^2\mathbb{E}[\|\mathbf{v}_{t-1}\|^2]}{\beta} + \frac{\beta C}{B} + \frac{\beta^2 C}{B}$$

Combining this inequality with lemma 1 and with  $\eta \leq O(\beta)$ , we can prove an optimization error

$$\mathbb{E}[\frac{1}{T} \sum_t \|\nabla F(\mathbf{w}_t)\|^2] \leq O(\frac{1}{\eta T} + \frac{1}{\beta T} + \frac{\beta}{B} + \frac{1}{\beta})$$

## F Proof of Theorem 3

The proof is similar to that of Theorem 2, except that the bound  $\Delta_t$ , which is shown below.

$$\begin{aligned}
\|\Delta_t\|^2 &= \|\mathbf{v}_t - \nabla F(\mathbf{w}_t)\|^2 \\
&= \left\| (1 - \beta)\mathbf{v}_{t-1} + \beta(\nabla F_1(\mathbf{w}_t; \mathcal{B}) + \frac{1}{B} \sum_{i \in \mathcal{B}} \nabla f([\mathbf{u}_t]_i) \nabla g_i(\mathbf{w}_t; \mathcal{A}, \mathcal{A}', \mathcal{B}_i)) - \nabla F(\mathbf{w}_t) \right\|^2 \\
&= \left\| \underbrace{(1 - \beta)(\mathbf{v}_{t-1} - \nabla F(\mathbf{w}_{t-1}))}_{A_1} + \underbrace{(1 - \beta)(\nabla F(\mathbf{w}_{t-1}) - \nabla F(\mathbf{w}_t))}_{A_2} \right. \\
&\quad \left. + \underbrace{\beta \left( \frac{1}{B} \sum_{i \in \mathcal{B}} \nabla f([\mathbf{u}_t]_i) \nabla g_i(\mathbf{w}_{t+1}; \mathcal{A}, \mathcal{A}', \mathcal{B}_i) - \frac{1}{B} \sum_{i \in \mathcal{B}} \nabla f(g_i(\mathbf{w}_t)) \nabla g_i(\mathbf{w}_t; \mathcal{A}, \mathcal{A}', \mathcal{B}_i) \right)}_{A_4} \right. \\
&\quad \left. + \underbrace{\beta \left( \nabla F_1(\mathbf{w}_t; \mathcal{B}) + \frac{1}{2B} \sum_{i \in \mathcal{B}} (\nabla f(g_i(\mathbf{w}_t)) \nabla g_i(\mathbf{w}_t; \mathcal{A}, \mathcal{B}_i) + \nabla f(g_i(\mathbf{w}_t)) \nabla g_i(\mathbf{w}_t; \mathcal{A}', \mathcal{B}_i)) - \nabla F(\mathbf{w}_t) \right)}_{A_5} \right\|^2.
\end{aligned}$$

from which we can see that  $A_3$  is gone in the proof of Theorem 2, which is the source to cause the error depends on  $\epsilon$ . Then we can follow the same analysis to finish the proof, which is omitted here due to that it is almost a duplicate of Theorem 2.

### F.1 Proof of Lemma 3

The proof is following that of Lemma 2 in [32]. We duplicate the proof here for completeness.

*Proof.* Based on Algorithm, the update rule of  $[\mathbf{u}]_i$  is

$$[\mathbf{u}_{t+1}]_i = \begin{cases} (1 - \gamma)[\mathbf{u}_t]_i + \gamma g_i(\mathbf{w}_{t+1}; \xi) & i \in \mathcal{B} \\ [\mathbf{u}_t]_i & i \notin \mathcal{B} \end{cases}.$$

where  $\xi$  denote the randomness in  $\mathcal{A}, \mathcal{A}', \mathcal{B}_i$ , and  $\mathbf{w}_{t+1} = \mathbf{w}_t$ . Below, we denote by  $B_1 = |\mathcal{B}|$  and  $\mathbb{E}[\|g_i(\mathbf{w}_{t+1}; \xi) - g_i(\mathbf{w}_{t+1})\|^2] \leq \frac{\sigma^2}{B_2}$ , where  $B_1 = B_2 = B = |\mathcal{B}|$ . We can re-write it into the equivalent expression below.

$$[\mathbf{u}_{t+1}]_i = \begin{cases} [\mathbf{u}_t]_i - \gamma ([\mathbf{u}_t]_i - g_i(\mathbf{w}_{t+1}; \xi)) & i \in \mathcal{B} \\ [\mathbf{u}_t]_i & i \notin \mathcal{B} \end{cases}. \quad (27)$$

Let us define  $\phi_t(\mathbf{u}) = \frac{1}{2} \|\mathbf{u} - \mathbf{g}(\mathbf{w}_t)\|^2 = \frac{1}{2} \sum_{i=1}^n \|\mathbf{u}_i - g_i(\mathbf{w}_t)\|^2$ , which is a 1-strongly convex function. Then, the update rule (27) can be viewed as one step of the stochastic block mirror descent algorithm (Algorithm 2 in [7]) for minimizing  $\phi_{t+1}(\mathbf{u})$ , where the Bregman divergence is defined by the quadratic function. Following the analysis of [7], we have

$$\begin{aligned}
\phi_{t+1}(\mathbf{u}_{t+1}) &= \frac{1}{2} \|\mathbf{u}_{t+1} - \mathbf{g}(\mathbf{w}_{t+1})\|^2 \\
&= \frac{1}{2} \|\mathbf{u}_t - \mathbf{g}(\mathbf{w}_{t+1})\|^2 + \langle \mathbf{u}_t - \mathbf{g}(\mathbf{w}_{t+1}), \mathbf{u}_{t+1} - \mathbf{u}_t \rangle + \frac{1}{2} \|\mathbf{u}_{t+1} - \mathbf{u}_t\|^2 \\
&= \frac{1}{2} \|\mathbf{u}_t - \mathbf{g}(\mathbf{w}_{t+1})\|^2 + \sum_{i \in \mathcal{B}} \langle [\mathbf{u}_t]_i - g_i(\mathbf{w}_{t+1}; \xi), [\mathbf{u}_{t+1}]_i - [\mathbf{u}_t]_i \rangle + \frac{1}{2} \sum_{i \in \mathcal{B}} \|[\mathbf{u}_{t+1}]_i - [\mathbf{u}_t]_i\|^2 \\
&\quad + \sum_{i \in \mathcal{B}} \langle g_i(\mathbf{w}_{t+1}; \xi) - g_i(\mathbf{w}_{t+1}), [\mathbf{u}_{t+1}]_i - [\mathbf{u}_t]_i \rangle.
\end{aligned}$$

Note that  $[\mathbf{u}_t]_i - g_i(\mathbf{w}_{t+1}; B_2) = ([\mathbf{u}_t]_i - [\mathbf{u}_{t+1}]_i)/\gamma$  and  $2 \langle b - a, a - c \rangle \leq \|b - c\|^2 - \|a - b\|^2 - \|a - c\|^2$ .

$$\begin{aligned}
& \sum_{i \in \mathcal{B}} \langle [\mathbf{u}_t]_i - g_i(\mathbf{w}_{t+1}; \xi), [\mathbf{u}_{t+1}]_i - [\mathbf{u}_t]_i \rangle \\
&= \sum_{i \in \mathcal{B}} \langle [\mathbf{u}_t]_i - g_i(\mathbf{w}_{t+1}; \xi), g_i(\mathbf{w}_{t+1}) - [\mathbf{u}_t]_i \rangle + \sum_{i \in \mathcal{B}} \langle [\mathbf{u}_t]_i - g_i(\mathbf{w}_{t+1}; \xi), [\mathbf{u}_{t+1}]_i - g_i(\mathbf{w}_{t+1}) \rangle \\
&= \sum_{i \in \mathcal{B}} \langle [\mathbf{u}_t]_i - g_i(\mathbf{w}_{t+1}; \xi), g_i(\mathbf{w}_{t+1}) - [\mathbf{u}_t]_i \rangle + \frac{1}{\gamma} \sum_{i \in \mathcal{B}} \langle [\mathbf{u}_t]_i - [\mathbf{u}_{t+1}]_i, [\mathbf{u}_{t+1}]_i - g_i(\mathbf{w}_{t+1}) \rangle \\
&\leq \sum_{i \in \mathcal{B}} \langle [\mathbf{u}_t]_i - g_i(\mathbf{w}_{t+1}; \xi), g_i(\mathbf{w}_{t+1}) - [\mathbf{u}_t]_i \rangle \\
&\quad + \frac{1}{2\gamma} \sum_{i \in \mathcal{B}} \left( \|[\mathbf{u}_t]_i - g_i(\mathbf{w}_{t+1})\|^2 - \|[\mathbf{u}_{t+1}]_i - [\mathbf{u}_t]_i\|^2 - \|[\mathbf{u}_{t+1}]_i - g_i(\mathbf{w}_{t+1})\|^2 \right)
\end{aligned}$$

If  $\gamma < \frac{1}{5}$ , we have

$$\begin{aligned}
& -\frac{1}{2} \left( \frac{1}{\gamma} - 1 - \frac{(\gamma+1)}{4\gamma} \right) \sum_{i \in \mathcal{B}} \|[\mathbf{u}_{t+1}]_i - [\mathbf{u}_t]_i\|^2 + \sum_{i \in \mathcal{B}} \langle g_i(\mathbf{w}_{t+1}; \xi) - g_i(\mathbf{w}_{t+1}), [\mathbf{u}_{t+1}]_i - [\mathbf{u}_t]_i \rangle \\
&\leq -\frac{1}{4\gamma} \sum_{i \in \mathcal{B}} \|[\mathbf{u}_{t+1}]_i - [\mathbf{u}_t]_i\|^2 + \gamma \sum_{i \in \mathcal{B}} \|g_i(\mathbf{w}_{t+1}; \xi) - g_i(\mathbf{w}_{t+1})\|^2 + \frac{1}{4\gamma} \sum_{i \in \mathcal{B}} \|[\mathbf{u}_{t+1}]_i - [\mathbf{u}_t]_i\|^2 \\
&= \gamma \sum_{i \in \mathcal{B}} \|g_i(\mathbf{w}_{t+1}; \xi) - g_i(\mathbf{w}_{t+1})\|^2.
\end{aligned}$$

Then, we have

$$\begin{aligned}
& \frac{1}{2} \|\mathbf{u}_{t+1} - \mathbf{g}(\mathbf{w}_{t+1})\|^2 \\
&\leq \frac{1}{2} \|\mathbf{u}_t - \mathbf{g}(\mathbf{w}_{t+1})\|^2 + \frac{1}{2\gamma} \sum_{i \in \mathcal{B}} \|[\mathbf{u}_t]_i - g_i(\mathbf{w}_{t+1})\|^2 - \frac{1}{2\gamma} \sum_{i \in \mathcal{B}} \|[\mathbf{u}_{t+1}]_i - g_i(\mathbf{w}_{t+1})\|^2 \\
&\quad + \gamma \sum_{i \in \mathcal{B}} \|g_i(\mathbf{w}_{t+1}; \xi) - g_i(\mathbf{w}_{t+1})\|^2 + \sum_{i \in \mathcal{B}} \langle [\mathbf{u}_t]_i - g_i(\mathbf{w}_{t+1}; \xi), g_i(\mathbf{w}_{t+1}) - [\mathbf{u}_t]_i \rangle \\
&\quad - \frac{(\gamma+1)}{8\gamma} \sum_{i \in \mathcal{B}} \|[\mathbf{u}_{t+1}]_i - [\mathbf{u}_t]_i\|^2.
\end{aligned}$$

Note that  $\frac{1}{2\gamma} \sum_{i \notin \mathcal{B}} \|[\mathbf{u}_t]_i - g_i(\mathbf{w}_{t+1})\|^2 - \frac{1}{2\gamma} \sum_{i \notin \mathcal{B}} \|[\mathbf{u}_{t+1}]_i - g_i(\mathbf{w}_{t+1})\|^2 = 0$  due to the update of  $\mathbf{u}_{t+1}$ , which implies that

$$\frac{1}{2\gamma} \sum_{i \in \mathcal{B}} \left( \|[\mathbf{u}_t]_i - g_i(\mathbf{w}_{t+1})\|^2 - \|[\mathbf{u}_{t+1}]_i - g_i(\mathbf{w}_{t+1})\|^2 \right) = \frac{1}{2\gamma_t} \left( \|\mathbf{u}_t - \mathbf{g}(\mathbf{w}_t)\|^2 - \|\mathbf{u}_{t+1} - \mathbf{g}(\mathbf{w}_t)\|^2 \right).$$

Besides, we also have:

$$\begin{aligned}
\mathbb{E}_t \left[ \sum_{i \in \mathcal{B}} \langle [\mathbf{u}_t]_i - g_i(\mathbf{w}_{t+1}; \xi), g_i(\mathbf{w}_{t+1}) - [\mathbf{u}_t]_i \rangle \right] &= \frac{B_1}{n} \sum_{i=1}^n \langle [\mathbf{u}_t]_i - g_i(\mathbf{w}_{t+1}), g_i(\mathbf{w}_{t+1}) - [\mathbf{u}_t]_i \rangle \\
&= -\frac{B_1}{n} \|\mathbf{u}_t - \mathbf{g}(\mathbf{w}_{t+1})\|^2 \\
\mathbb{E} \left[ \sum_{i \in \mathcal{B}} \|g_i(\mathbf{w}_{t+1}; \xi) - g_i(\mathbf{w}_{t+1})\|^2 \right] &\leq \frac{B_1 \sigma^2}{B_2}.
\end{aligned}$$

Then, we can obtain

$$\frac{\gamma+1}{2} \mathbb{E} \left[ \|\mathbf{u}_{t+1} - \mathbf{g}(\mathbf{w}_{t+1})\|^2 \right] \leq \frac{\gamma \left( 1 - \frac{B_1}{n} \right) + 1}{2} \mathbb{E} \left[ \|\mathbf{u}_t - \mathbf{g}(\mathbf{w}_{t+1})\|^2 \right] + \frac{\gamma^2 B_1 \sigma^2}{B_2} - \frac{(\gamma+1)}{8} \sum_{i \in \mathcal{B}} \|[\mathbf{u}_{t+1}]_i - [\mathbf{u}_t]_i\|^2.$$

Further dividing by  $\frac{\gamma+1}{2}$  and taking full expectation on both sides

$$\mathbb{E} \left[ \|\mathbf{u}_{t+1} - \mathbf{g}(\mathbf{w}_{t+1})\|^2 \right] \leq \frac{\gamma \left(1 - \frac{B_1}{n}\right) + 1}{\gamma + 1} \mathbb{E} \left[ \|\mathbf{u}_t - \mathbf{g}(\mathbf{w}_{t+1})\|^2 \right] + \frac{2}{1 + \gamma} \frac{\gamma^2 \sigma^2 B_1}{B_2} - \frac{1}{4} \mathbb{E} \left[ \sum_{i \in \mathcal{B}} \|[\mathbf{u}_{t+1}]_i - [\mathbf{u}_t]_i\|^2 \right].$$

Note that  $\frac{\gamma(1 - \frac{B_1}{n}) + 1}{\gamma + 1} = 1 - \frac{\gamma B_1}{(\gamma + 1)n} \leq 1 - \frac{\gamma B_1}{2n}$  and  $\frac{1}{1 + \gamma} \leq 1$  for  $\gamma \in (0, 1]$ . In addition, we have  $\|\mathbf{u}_t - \mathbf{g}(\mathbf{w}_{t+1})\|^2 \leq (1 + \frac{\gamma B_1}{4n}) \|\mathbf{u}_t - \mathbf{g}(\mathbf{w}_t)\|^2 + (1 + \frac{4n}{\gamma B_1}) \|\mathbf{g}(\mathbf{w}_{t+1}) - \mathbf{g}(\mathbf{w}_t)\|^2$  due to Young's inequality and  $\|\mathbf{g}(\mathbf{w}_t) - \mathbf{g}(\mathbf{w}^{t-1})\|^2 \leq nC_g^2 \|\mathbf{w}_{t+1} - \mathbf{w}_t\|^2 = n\eta^2 C_g^2 \|\mathbf{v}^t\|^2$ .

$$\begin{aligned} \mathbb{E} [\Xi_{t+1}] &= \mathbb{E} \left[ \frac{1}{n} \|\mathbf{u}_{t+1} - \mathbf{g}(\mathbf{w}_{t+1})\|^2 \right] \\ &\leq \left(1 - \frac{\gamma B_1}{2n}\right) \mathbb{E} \left[ \frac{1}{n} \|\mathbf{u}_t - \mathbf{g}(\mathbf{w}_{t+1})\|^2 \right] + \frac{2\gamma^2 \sigma^2 B_1}{nB_2} - \frac{1}{4n} \mathbb{E} \left[ \sum_{i \in \mathcal{B}} \|[\mathbf{u}_{t+1}]_i - [\mathbf{u}_t]_i\|^2 \right] \\ &\leq \left(1 - \frac{\gamma B_1}{2n}\right) \left(1 + \frac{\gamma B_1}{4n}\right) \mathbb{E} \left[ \frac{1}{n} \|\mathbf{u}_t - \mathbf{g}(\mathbf{w}_t)\|^2 \right] + \frac{5nC_g^2 \mathbb{E} [\|\mathbf{w}_{t+1} - \mathbf{w}_t\|^2]}{\gamma B_1} + \frac{2\gamma^2 \sigma^2 B_1}{nB_2} \\ &\quad - \frac{1}{4n} \mathbb{E} \left[ \sum_{i \in \mathcal{B}} \|[\mathbf{u}_{t+1}]_i - [\mathbf{u}_t]_i\|^2 \right] \\ &\leq \left(1 - \frac{\gamma B_1}{4n}\right) \mathbb{E} [\Xi_t] + \frac{5n\eta^2 C_g^2 \mathbb{E} [\|\mathbf{v}^t\|^2]}{\gamma B_1} + \frac{2\gamma^2 \sigma^2 B_1}{nB_2} - \frac{1}{4n} \mathbb{E} \left[ \sum_{i \in \mathcal{B}} \|[\mathbf{u}_{t+1}]_i - [\mathbf{u}_t]_i\|^2 \right]. \end{aligned}$$

□